



UNITED STATES
NUCLEAR REGULATORY COMMISSION
WASHINGTON, D. C. 20555

PDR

APR 25 1980

MEMORANDUM FOR: Harold R. Denton, Director
Office of Nuclear Reactor Regulation

FROM: Robert J. Budnitz, Director
Office of Nuclear Regulatory Research

SUBJECT: RESEARCH INFORMATION LETTER # 88, "DESIGN
CRITERIA FOR CLOSELY-SPACED NOZZLES IN PRESSURE
VESSELS"

This memorandum transmits the results of completed research dealing with the establishment of design criteria for closely-spaced nozzles in pressure vessels and the resulting change to the ASME Code rules (Appendix A). Seven reports (Appendices B through H) issued in the process of this research are enclosed. The eighth and final report (Appendix I) is in the process of publication and will be submitted upon completion.

1.0 Introduction

The results described herein were generated in a research program whose objectives were to investigate the state-of-stress at reinforced openings (nozzles) in cylindrical pressure vessels operating at temperatures below the creep range, such as for light water reactor (LWR) vessels, and to assess the rules and criteria that govern the design and qualification of isolated and closely-spaced nozzles in reactor vessels. Two of the more important parameters investigated are the maximum stresses in the nozzle-vessel region and the minimum distance between nozzles or between a nozzle and other structural discontinuity. These must be limited to acceptable values to assure that the vessel will not develop failure mechanisms from excessive peak stresses (initiation of fatigue cracks) and from high local membrane stresses (excessive distortion due to material yielding). Although the ASME Boiler and Pressure Vessel Code, Section III, Nuclear Power Plant Components, contains clear instructions for designing nozzle penetrations including geometric details, reinforcement rules, stress indices, and spacing requirements, there was concern that the Code rules for computing maximum stresses (stress indices) and for maintaining an appropriate distance between nozzles to prevent excessive interaction of stress fields were inadequate, at least over some range of the geometric parameters covered by the rules. There was also a desire to reduce the minimum spacing distances in the event that the present criteria are overly conservative.

12055011853 999 LL
US NRC
RES
OFFICE DIRECTOR
1130SS
WASHINGTON

DC 20555

8107150387 800425

PDR RES

8107150387

PDR

2.0 Discussion

In order to investigate these questions, ORNL developed and validated two special purpose finite-element stress analysis computer programs, CORTES and MULT-NOZZLE, for analyzing pressure vessels with a single (isolated) nozzle or with two or more closely-spaced nozzles, under loading conditions of internal pressure and/or force and moments applied to the end(s) of the nozzle(s). These computer programs were used to conduct parametric studies of the ASME Code endorsed nozzle designs over a wide range of dimensionless geometric parameters. Work was carried out to correlate the calculated maximum stress data developed with experimental data and to compare these correlations with the ASME Code calculated stress indices. The information developed as described above led to the establishment of a new criterion for defining an "isolated nozzle condition." And finally, the work carried out led to the development of proposed alternate criteria, both for computing the maximum stress intensity (not to be confused with the stress intensity of fracture mechanics terminology) for a given nozzle design and loading condition and for limiting the maximum distance between nozzles. These criteria are given in a form that can be introduced into the ASME Code to replace the present rules.

3.0 Results

Results of the studies (see Appendix G) show that the Code stress index for computing the maximum design stress intensity at the inside corner of the nozzle-vessel junction can be unconservative for values of the parametric relation:

$$\eta = (d_i/D_i)^{0.133} (D_i/T)^{0.18} > 1.1 \quad (1)$$

where d_i = inside diameter of nozzle

D_i = inside diameter of vessel

T = actual wall thickness of vessel minus corrosion allowance.

The degree of this unconservatism is dependent upon the amount and placement of nozzle reinforcement material allowed by the latitude permitted by Code reinforcement rules. Since many (or most of the

reactor vessel designs of current interest have values of the parameter η , less than 1.1, it is recommended that use of the current Code indices be limited to values of $\eta < 1.1$. This is somewhat more restrictive than the present Code limit of:

$$\rho = (d_i/D_i)\sqrt{D_i/T} < 0.8 \quad (2)$$

For nozzle designs with $\eta > 1.1$, such as occur routinely in piping applications, more elaborate stress index formulas were developed for both internal pressure and applied moment loadings to replace the present Code indices. These recommendations, in the form of proposed Code rule revisions, have been presented to the ASME Boiler and Pressure Vessel Code Committee and are summarized in Appendix A.

Results of the studies addressed to the question of nozzle spacing (see Appendix I - to be supplied at a later date) indicate that the Code rules are inadequate in several respects, primarily due to the lack of a sufficient data base. Nozzle spacing rules as given in various portions of the Code are not consistent. Of more importance, however, is the fact that a given rule may be conservative in one respect, such as for nozzles spaced around the circumference of a vessel, but unconservative in another respect, such as for nozzles spaced in a longitudinal plane or in some nonorthogonal plane. Further, the Code rules may be unconservative for smaller nozzles with all the required reinforcement placed in the nozzle wall but excessively conservative for larger nozzles with a significant portion of the reinforcement in the form of increased vessel wall thickness.

To resolve these problems two items were needed: (1) an acceptable definition of the isolated nozzle condition in terms of the dimensional extent of the region in which the nozzle has a significant influence on the primary membrane stresses in the vessel, and (2) a computational rule for limiting the minimum distance between nozzles so that their local primary membrane stresses regions do not interact significantly. To define the isolated nozzle condition, the criterion that a primary membrane stress intensity greater than 10 percent above nominal would be considered significant, and that the directional distance from the nozzle centerline to the 1.1 T_{nom} contour would be considered the boundary of the isolated nozzle region was adopted. The region was then further defined in terms of the dimensional parameters of the nozzle and vessel, the directional

orientation of the nozzles, and a vessel-wall reinforcement parameter, based on analytical results obtained from the finite-element parameter studies and existing experimental data.

A new nozzle spacing rule based on the additional condition that no two nozzles should be closer than the sum of the distances to the boundary of their respective isolated nozzle has been formulated. This new rule is being proposed as a replacement for the four or more rules in current use. Figure 1, extracted from Appendix I (report not yet available) shows a comparison between the longitudinal spacing requirement of the new rule and the current rules for Class 1 nuclear pressure vessels (and piping) as a function of the nondimensional parameter.

$$\lambda = (d_1 + d_2) / \sqrt{R_i T_r} \quad (3)$$

where d_1, d_2 = inside diameters of nozzles

R_i = inside radius of the vessel (or pipe)

T_r = minimum vessel wall thickness required by Code to resist design pressure.

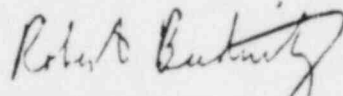
The new rule, which includes the influence of the additional nondimensional parameters D_i/T_a , t_n/T_a and T_a/T_r , where D_i is the inside diameter of the vessel, T_a is the actual vessel wall thickness, and t_n is the nozzle wall thickness, is illustrated for parametric values of $D_i/T_a = 10$ and 100 and $T_a/T_r = 1$ and 2 . This range effectively brackets the range of current pressure vessel design. Values of t_n/T_a were chosen to satisfy the Code rules for 100 percent reinforcement specified in paragraph NP-3338 of Section III of the Code.

Figure 1 (enclosure 1) shows that although the current rules are simpler, since they are expressed only in terms of the one parameter λ , they are somewhat unconservative for values of $\lambda < 2.75$ (which includes most nuclear applications) when $T_a/T_r = 1$. On the other hand, when the nozzle course of the vessel is thicker than the minimum required, i.e., $T_a/T_r > 1$ and/or when $\lambda > 2.75$ (which includes most piping installations), the current rules tend to be excessively conservative. Thus, application of the new rule will not only contribute to an increase in effective margins of safety but will also allow for design options that are not available under the current rules without detailed and expensive analyses.

4.0 Recommendations and Conclusions

The proposed Code revisions for nozzle spacing and for stress indices for nuclear Class 1 vessels [NB-3300, NB-3338.2(d)(3) and NB-3339.1(f)] and nuclear Class 1 piping branch connections [NB-3600 and NB-3683.8] are enclosed as Appendix A. The latter are given in the proposed complete rewrite of the present ASME Code paragraph NB-3683 and stress index table [Table NB-3681(a)-1].

The impact of this research program, leading to better design rules for vessel-nozzle, piping-branch design, does not require any reexamination of existing configurations. Such configurations have been traditionally designed with wall thicknesses in excess of Code minimums and, where they have been designed to Code minimums, the resultant modest decrease in safety factors, as shown in this program, does not compromise the safety of the structures in question. This is due to the large inherent factors of safety built in the Code directly, particularly as apply to stress limits for the approved vessel, nozzle and piping material.

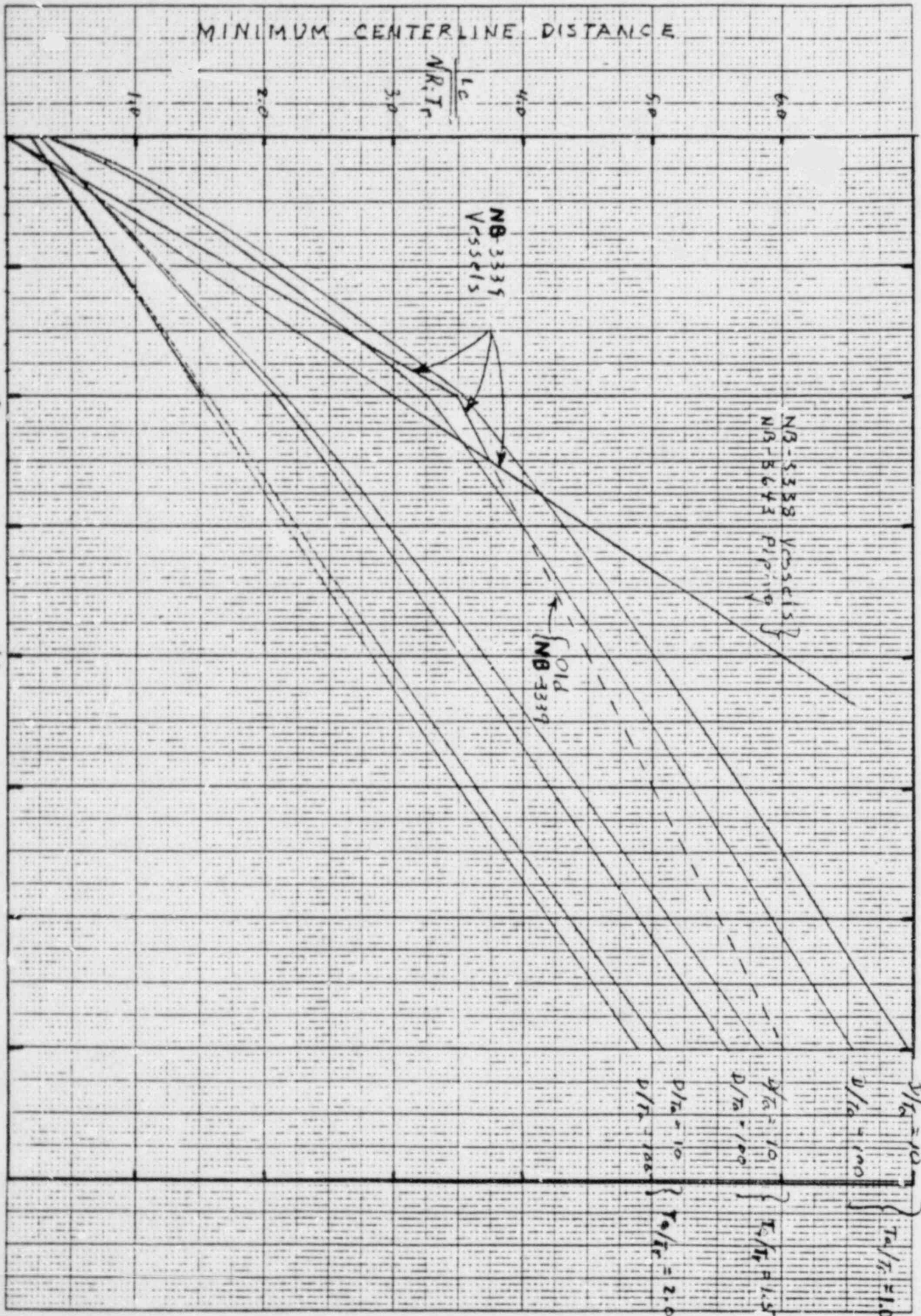


Robert J. Budnitz, Director
Office of Nuclear Regulatory Research

Enclosures:

1. Figure 1
2. Appendices A-H
(see attached sheet)

MINIMUM CENTERLINE DISTANCE



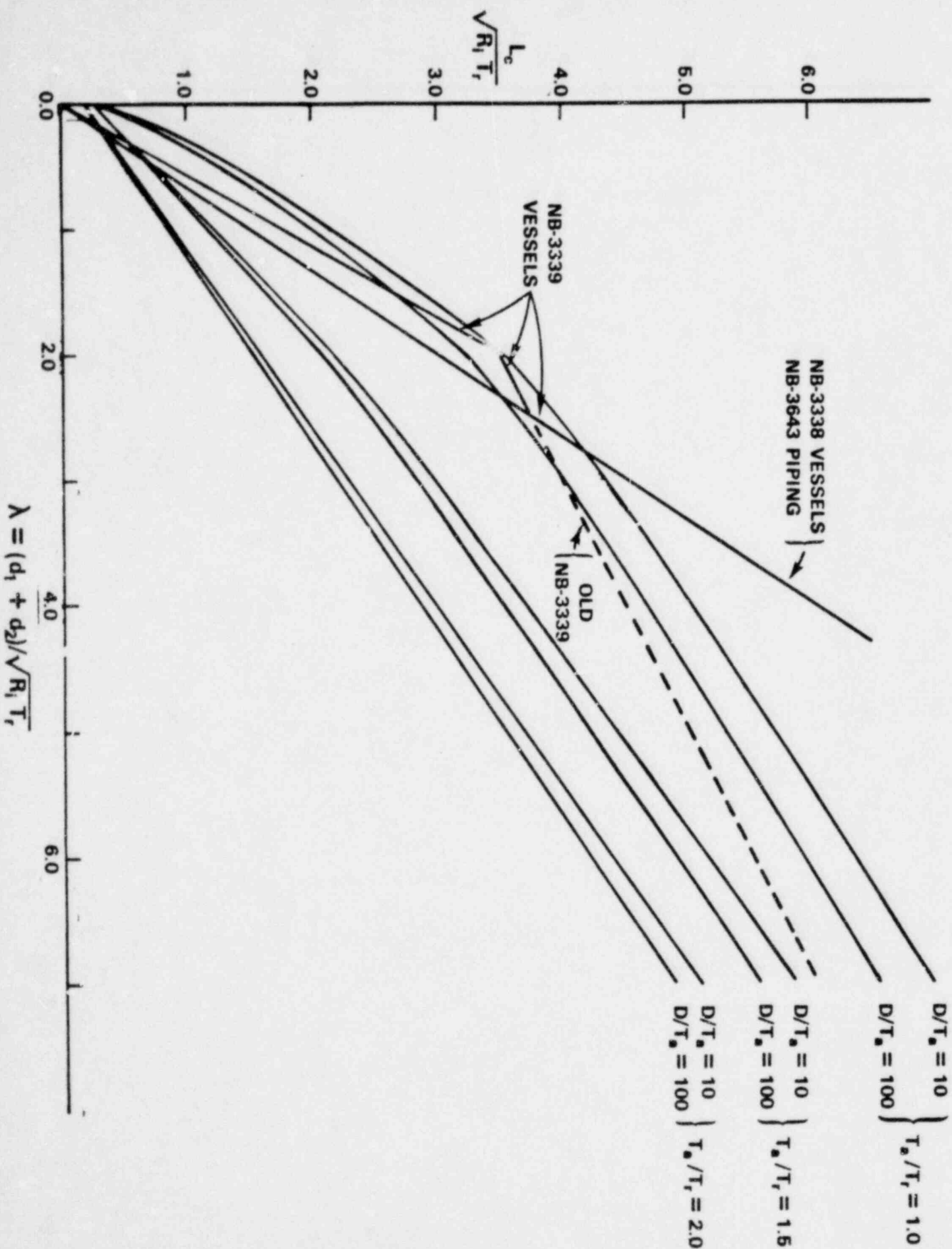
$$\lambda = (d_1 + d_2) / \sqrt{R_i T_i}$$

Fig. 1. Proposed minimum normalized center line-to-center line distance $L_C/\sqrt{R_i T_p}$ between nozzles in a longitudinal plane of a nuclear class 1 cylindrical pressure vessel or straight pipe as a function of the dimensionless sum-of-inside-diameters parameter $\lambda = (d_1 + d_2)/\sqrt{R_i T_p}$, where L_C is the centerline distance measured along the inside surface of the shell, R_i is the inside radius of the vessel (or pipe), T_p is the minimum required wall thickness of the vessel computed by the equations given in Code paragraphs NB-3324.1 or NB-3641.1. The lines identified by parametric values, e.g., $D/T_a = 10$, $T_a/T_p = 1$ are plots of the proposed rule for various values of the vessel inside diameter-to-actual wall thickness ratio D/T_a and the excess vessel thickness parameter T_a/T_p . The lines identified by Code paragraph number, NB-3338, NB-3339, and NB-3643 are plots of the current rules under the subject paragraph. The dashed line (old NB-3339) is the so-called $2\frac{1}{2}\sqrt{RT}$ rule given in the Code prior to the 1977 edition.

Appendices

- A. Proposed Revisions to ASME Boiler and Pressure Vessel Code, Section III, Paragraphs NB-3300, NB-3338.2(d)(3), NB-3339.1(f), NB-3600, NB-3683.8 and Table NB-3681(a)-1
- B. B. R. Bass, J. W. Bryson, and S. E. Moore, "Validation of the Finite Element Stress Analysis Computer Program CORTES-SA for Analyzing Piping Tees and Pressure Vessel Nozzles," Pressure Vessels and Piping Computer Program Evaluation and Qualification, PVP-PB-024, pp. 9-25, ASME (1977)
- C. J. W. Bryson, W. G. Johnson, and B. R. Bass, "Stresses in Reinforced Nozzle-Cylinder Attachments Under Internal Pressure Loading Analyzed by the Finite-Element Method - A Parameter Study," ORNL/NUREG-4 (October 1977)
- D. F. K. W. Tso et al., "Stress Analysis of Cylindrical Pressure Vessels with Closely Spaced Nozzles by the Finite-Element Method, Volume 1. Stress Analysis of Vessels with Two Closely Spaced Nozzles Under Internal Pressure," ORNL/NUREG-18/V1 (November 1977)
- E. F. K. W. Tso and R. A. Weed, "Stress Analysis of Cylindrical Pressure Vessels with Closely Spaced Nozzles by the Finite-Element Method, Volume 2. Vessels with Two Nozzles Under External Force and Moment Loadings," NUREG/CR-0123, ORNL/NUREG-18/V2 (August 1978)
- F. F. K. W. Tso and R. A. Weed, "Stress Analysis of Cylindrical Pressure Vessels with Closely Spaced Nozzles by the Finite-Element Method, Volume 3. Vessels with Three Nozzles Under Internal Pressure and External Loadings," NUREG/CR-0507, ORNL/NUREG-18/V3 (May 1979)
- G. E. C. Rodabaugh and S. E. Moore, "Stress Indices and Flexibility Factors for Nozzles in Pressure Vessels and Piping," NUREG/CR-0778, ORNL/Sub-2913/10 (June 1979)
- H. J. W. Bryson, W. G. Johnson, and B. R. Bass, "Stresses in Reinforced Nozzle-Cylinder Attachments Under External Moment Loadings Analyzed by the Finite-Element Method - A Parameter Study," NUREG/CR-0506, ORNL/NUREG-52 (August 1979)
- I. S. E. Moore and J. L. Mershon, "Design Criteria for the Spacing of Nozzles and Reinforced Openings in Cylindrical Class 1 Nuclear Pressure Vessels," (Draft)

MINIMUM CENTERLINE DISTANCE



APPENDIX A

PROPOSED ASME CODE RULES MODIFICATIONS RELATIVE TO NOZZLE SPACING IN NUCLEAR CLASS 1 PRESSURE VESSELS AND PIPING

Class 1 Vessels (NB-3300)

- 1. Delete the last sentence of NB-3331(d) . . . "If fatigue analysis is not required, the restrictions on hole spacing are applicable unless there will be essentially no pipe reactions."
- 2. Add a new subsubparagraph to NB-3331:

NB-3331(h) For openings in a spherical shell or head, the arc distance measured between the center lines of adjacent nozzles along the inside surface of the shell shall be not less than two times the sum of their inside radii. For openings in a cylindrical shell, their centerline distance along the inside surface of the shell shall be such that $[(L_c/2)^2 + (L_\lambda/3)^2]^{1/2}$ is not less than F_c times the sum of their inside radii, where

$$F_c = 4e^{-C_1 t/t_n (D/t)^{-0.075}} (t_n/t)^{0.1} \lambda^{C_2 t/t_n - C_3} + \frac{1}{3} [1 + (0.4 - 0.1 t/t_n)/\lambda] ,$$

$$\lambda = (d_1 + d_2) / 2\sqrt{Rt_n} ,$$

$$t_n = \frac{1}{2}(t_{n1} + t_{n2}) ,$$

and where the magnitude of t/t_n used in computing the minimum nozzle spacing is not greater than 2.0. Numerical values of the constants C_1 , C_2 , and C_3 are tabulated below for the appropriate range of λ :

λ	C_1	C_2	C_3
0 to 1	1.53	0.20	0.53
1 to 3	1.53	0.62	1.39
3 to 8	1.46	0.62	1.43

If t/t_n is greater than 1.0, the thickened portion of the vessel shall extend a distance from the center line of either nozzle not less than $3F_c$ times the diameter of the larger nozzle in the longitudinal direction and not less than $2F_c$ times the diameter of the larger nozzle in the circumferential direction. Symbols used in the computations for minimum nozzle spacings are defined as follows:

D = inside diameter, in the corroded condition, of the vessel shell, in.

d_1, d_2 = inside diameters, in the corroded condition, of the two openings under consideration, in.

F_c = a correction factor which compensates for the membrane stress attenuation in the vessel as a function of nozzle dimensions.

$R = 1/2 D =$ inside radius of the vessel shell, in.

$t =$ wall thickness of the vessel shell in the region of the opening, in.

$t_r =$ thickness of the vessel shell which meets the requirements of NB-3221.1 in the absence of the opening, in.

$t_{n1}, t_{n2} =$ thicknesses of the two nozzles under consideration (see Fig. NB-3338.2-2), in.

$\lambda =$ nondimensional stress attenuation parameter.

3. Replace NB-3332.1(b) with the following:

NB-3332.1(b). No two unreinforced openings shall have their centers closer to each other, measured along the inside surface of the vessel wall, than $0.3\sqrt{Rt_r}$ plus 2.4 times the sum of their diameters.

4. Replace NB-3338.2(d)(2) with the following:

NB-3338.2(d)(2). The arc distance measured between the center lines of adjacent nozzles meets the requirements of NB-3331(h).

5. Replace NB-3339.1(d) with the following:

NB-3339.1(d). The arc distance measured between the centerlines of adjacent nozzles meets the requirements of NB-3331(h).

Class 1 Piping (NB-3600)

1. Add a new subsubparagraph to NB-3643.1:

NB-3643.1(g). For branch connections in a pipe, the arc distance measured between the centerlines of adjacent branches along the outside surface of the run pipe shall be such that $[(L_1/2)^2 + (L_2/3)^2]^{1/2}$ is not less than F_c times the sum of their inside radii, where

$$F_c = 4e^{-C_1 T_r / t_m} \left(\frac{D_o - 2T_r}{T_r} \right)^{-0.075} \left(\frac{T_{b1} + T_{b2}}{2 T_r} \right)^{0.1} \lambda^{C_2 T_r / t_m - C_3} + \frac{1}{3} \left[1 + \frac{0.4 - 0.1 T_r / t_m}{\lambda} \right],$$

$$\lambda = (d_1 + d_2) / \sqrt{2(D_o - 2T_r)t_m}.$$

Numerical values of the constants C_1 , C_2 , and C_3 are tabulated below for the appropriate range of λ :

λ	C_1	C_2	C_3
0 to 1	1.53	0.20	0.53
1 to 3	1.53	0.62	1.39
3 to 8	1.46	0.26	1.43

2. Replace NB-3643.3(b)(1)(b) with the following:
(b) No two unreinforced openings shall have their centers closer together, measured on the outside surface of the run pipe, than $0.3\sqrt{0.5(D_o - 2T_m)t_m}$ plus 2.4 times the sum of their diameters.
3. Replace new NB-3683.8(a)(1) with the following:
(1) For branch connections in a pipe, the arc distance measured between the centers of adjacent branches meets the requirements of NB-3643.1(g).

for hillside connections in spheres or cylinders

$$K_2 = K_1 (1 + 2 \sin^2 \varphi)$$

for lateral connections in cylinders

$$K_2 = K_1 [1 + (\tan \varphi)^{4/3}]$$

where

K_1 = the σ_n inside stress index of Table NB-3338.2(c)-1 for a radial connection

K_2 = the estimated σ_n inside stress index for the nonradial connection

W78 (2) The arc distance measured between the center lines of adjacent nozzles along the inside surface of the shell is not less than three times the sum of their inside radii for openings in a head or along the longitudinal axis of a shell and is not less than two times the sum of their radii for openings along the circumference of a cylindrical shell. When two nozzles in a cylindrical shell are neither in a longitudinal line nor in a circumferential arc, their center line distance along the inside surface of the shell shall be such that $[(L_c/2)^2 + (L_l/3)^2]^{1/2}$ is not less than the sum of their inside radii, where L_c is the component of the center line distance in the circumferential direction and L_l is the component of the center line distance in the longitudinal direction.

S77 (3) The dimensional ratios are not greater than the following:

Ratio	Cylinder	Sphere
$\frac{\text{Inside shell diameter}}{\text{Shell thickness}} = \frac{D}{t}$	100	100
$\frac{\text{Inside nozzle diameter}}{\text{Inside shell diameter}} = \frac{d}{D}$	0.50	0.50
$\frac{d}{\sqrt{Dt}}$	0.80 1.1	0.80

$(D/D) 0.133$ $(D/t) 0.188$

In the case of cylindrical shells, the total nozzle reinforcement area on the transverse axis of the connections including any outside of the reinforcement limits, shall not exceed 200% of that required for the longitudinal axis (compared to 50% permitted by Fig. NB-3332.2-1) unless a tapered transition section is incorporated into the reinforcement and the shell, meeting the requirements of NB-3361.

(4) In the case of spherical shells and formed heads, at least 40% of the total nozzle reinforcement area shall be located beyond the outside surface of the minimum required vessel wall thickness.

(5) The inside corner radius, r_1 (Fig. NB-3338.2-2), is between 10% and 100% of the shell thickness, t .

(6) The outer corner radius, r_2 (Fig. NB-3338.2-2), is large enough to provide a smooth transition between the nozzles and the shell. In addition, for

opening diameters greater than 1½ times shell thickness in cylindrical shells and 2:1 ellipsoidal heads and greater than three shell thicknesses in spherical shells, the value of r_2 shall be not less than one-half the thickness of the shell or nozzle wall, whichever is greater.

(7) The radius, r_2 (Fig. NB-3338.2-2), is not less than the greater of the following:

(a) $0.002 \theta d_o$, where d_o is the outside diameter of the nozzle and is as shown in Fig. NB-3338.2-2, and the angle θ is expressed in degrees;

(b) $2(\sin \theta)^3$ times offset for the configuration shown in Figs. NB-3338.2-2(a) and (b).

NB-3339 Alternative Rules for Nozzle Design

Subject to the limitations stipulated in NB-3339.1, the requirements of this paragraph constitute an acceptable alternative to the rules of NB-3332 through NB-3336 and NB-3338.

NB-3339.1 Limitations. These alternative rules are applicable only to nozzles in vessels within the limitations stipulated in (a) through (f) below.

(a) The nozzle is circular in cross section and its axis is normal to the vessel or head surface.

(b) The nozzle and reinforcing (if required) are welded integrally into the vessel with full penetration welds. Details such as those shown in Figs. NB-4244(a)-1, NB-4244(b)-1 and NB-4244(c)-1 are acceptable. However, fillet welds shall be finished to a radius in accordance with Fig. NB-3339.1-1.

(c) In the case of spherical shells and formed heads, at least 40% of the total nozzle reinforcement area shall be located beyond the outside surface of the minimum required vessel wall thickness.

(d) The spacing between the edge of the opening and the nearest edge of any other opening is not less than the smaller of $1.25(d_1 + d_2)$ or $2.5\sqrt{Rt}$, but in any case not less than $d_1 + d_2$. d_1 and d_2 are the inside diameters of the openings.

(e) The material used in the nozzle, reinforcing, and vessel adjacent to the nozzle shall have a ratio of UTS/YS of not less than 1.5 where

UTS = specified minimum ultimate tensile strength

YS = specified minimum yield strength

(f) The following dimensional limitations are met:

	Nozzles in Cylindrical Vessels	Nozzles in Spherical Vessels or Hemispherical Heads
D/d	10 to 200	10 to 100
d/D	0.33 max.	0.5 max.
d/Dt	0.133	0.8 max.

S77
W79

S77
W79

$(d/D)^{0.133}$ $(D/t)^{0.133}$ 1.1

Outline for NB-3683

NB-3683 STRESS INDICES FOR USE WITH NB-3650

- NB-3683.1 Nomenclature
 - (a) Dimensions
 - (b) Material properties
 - (c) Connecting welds
 - (d) Loadings
- NB-3683.2 Applicability of Indices - General
 - (a) Abutting products
 - (b) Out-of-round products
- NB-3683.3 Straight Pipe Remote from Welds
- NB-3683.4 Connecting Welds
 - (a) Longitudinal butt welds
 - (b) Girth butt welds
 - (c) Girth fillet welds
- NB-3683.5 Welded Transitions
 - (a) NB-4250 transitions
 - (b) Transitions within a 1:3 slope
- NB-3683.6 Concentric Reducers
 - (a) Primary plus secondary stress indices
 - (b) Peak stress indices
- NB-3683.7 Curved Pipe or Butt-Welding Elbows
 - (a) Primary stress index
 - (b) Primary plus secondary stress indices
- NB-3683.8 Branch Connections per NB-3643
 - (a) Applicability
 - (b) Primary stress indices
 - (c) Primary plus secondary stress indices
 - (d) Peak stress indices
- NB-3683.9 Butt Welding Tees
 - (a) Primary stress indices
 - (b) Primary plus secondary stress indices
 - (c) Peak stress indices

NB-3683 STRESS INDICES FOR USE WITH NB-3650

The stress indices given herein and in Table NB-3681(a)-1, and subject to the additional restrictions specified herein are to be used with the analysis methods of NB-3650. For piping products outside the applicable range, stress indices shall be established in accordance with NB-3681.

NB-3683.1 Nomenclature

(a) *Dimensions.* Nominal dimensions as specified in the dimensional standards of Table NB-3132.1 shall be used for calculating the numerical values of the stress indices given herein and in Table NB-3681(a)-1 and for evaluating Eqs. (9) through (14) of NB-3650. For ANSI B16.9, ANSI B16.28, MSS SP 48 or MSS SP 87 piping products, the nominal dimensions of the equivalent pipe, e.g., sched. 40, as certified by the manufacturer, shall be used. Not more than one equivalent pipe size shall be certified for given product items of the same size, shape, and weight.

For piping products such as reducers and tapered-wall transitions which have different dimensions at either end, the nominal dimensions of the large or small end, whichever gives the larger value of D_o/t shall be used. Dimensional terms are defined as follows.

- D_o = nominal outside diameter of pipe, in.
- D_i = nominal inside diameter of pipe, in.
- D_m = $2R_m = (D_o - T_n)$ = mean diameter of designated run pipe, in. See NB-3683.8(c) and Fig. NB-3683.3(a)-1.
- D_{max} = maximum outside diameter of cross section, in.
- D_{min} = minimum outside diameter of cross section, in.
- D_1 = nominal outside diameter at large end of concentric reducer, in. See NB-3683.6.
- D_2 = nominal outside diameter at small end of concentric reducer, in. See NB-3683.6.
- d_o = nominal outside diameter of attached branch pipe, in.
- d_i = nominal inside diameter of branch, in.
- d_m = $(d_i + t_n)$ = nominal mean diameter of reinforced or unreinforced branch, in. See NB-3683.8(c).
- h = tR/n^2 = characteristic bend parameter of a curved pipe or butt-welding elbow.
- I = $0.0491 (D_o^4 - D_i^4)$ = moment of inertia of pipe, in.

- L_1 = height of nozzle reinforcement for branch connections, in. See Fig. NB-3643.3(a)-1.
- L_1, L_2 = length of cylindrical portion at the large end and small end of a reducer, respectively. See NB-3683.6.
- R = nominal bend radius of curved pipe or elbow, in.
- R_m = $(D_o - T_r)/2$ = mean radius of designated run pipe, in. See NB-3683.8 and Fig. NB-3643.3(a)-1.
- r_i = $d_i/2$ = inside radius of branch, in. See Fig. NB-3643.3(a)-1.
- r_m = $(D_o - t)/2$ = mean pipe radius, in.
- r'_m = $(d_o - T'_b)/2$ = mean radius of attached branch pipe, in., see Fig. NB-3643.3(a)-1.
- r_p = outside radius of reinforced nozzle or branch connection, in. See Fig. NB-3643.3(a)-1.
- r_1, r_2, r_3 = designated radii for reinforced branch connections and concentric reducers, in., see NB-3683.6, NB-3683.8, and Fig. NB-3643.3(a)-1.
- T_b = nominal wall thickness of attached branch pipe, in., see Fig. NB-3643.3(a)-1.
- T'_b = wall thickness of branch connection reinforcement, in., see Fig. NB-3643.3(a)-1.
- T_r = nominal wall thickness of designated run pipe, in., see Fig. NB-3643.3(a)-1.
- t = nominal wall thickness of pipe, in. For piping products purchased to a minimum wall specification, the nominal wall thickness shall be taken as 1.14 times the minimum wall.
- t_n = wall thickness of nozzle or branch connection reinforcement, in. See NB-3683.8; also used for concentric reducers, see NB-3683.6.
- t_{max} = maximum wall thickness of a welding transition within a distance of $\sqrt{D_o t}$ from the welding end. See NB-3683.5(b).
- t_1 = nominal wall thickness at large end of concentric reducer, in. See NB-3683.6.
- t_2 = nominal wall thickness at small end of concentric reducer, in. See NB-3683.6.
- t_{1m}, t_{2m} = minimum wall thicknesses at the large end and small end of a reducer, respectively that is required to resist the design pressure P in accordance with Eq. (1), NB-3641.1.

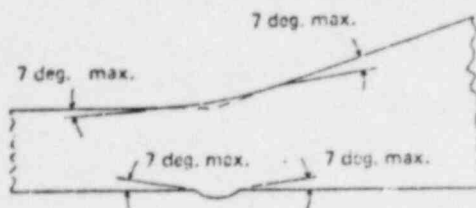
- $Z = 2I/D_o =$ section modulus at pipe, in.³
 $Z_b = \pi(r'_m)^2 T'_b =$ approximate section modulus of attached branch pipe, in.³
 $Z_r = \pi(R'_m)^2 T'_r =$ approximate section modulus of designated run pipe, in.³
 $\alpha =$ cone angle of concentric reducer, deg. per NB-3683.6.
 $\delta =$ the average permissible mismatch at girth butt welds as shown in Fig. NB-4233-1. A value of δ less than 1/32 in. may be used provided that the smaller mismatch is specified for fabrication. For "flush" welds as defined in NB-3683.1(a) and for $t > 0.237$ in., δ may be taken as zero.
 $\Delta =$ radial weld shrinkage measured from the nominal outside surface, in.
 $\theta =$ slope of nozzle-to-pipe transition for branch connections, degrees. See Fig. NB-3643.3(a)-1.

(b) *Material Properties.* Unless otherwise specified, materials properties at the appropriate temperature, as given in Appendix I shall be used. Terms are defined as follows.

- $E =$ modulus of elasticity for the material at room temperature, psi, taken from Table I-6.0.
 $M =$ materials constant.
 $= 2$ for ferritic steels and nonferrous materials except nickel-chrome-iron alloys and nickel-iron-chrome alloys.
 $= 2.7$ for austenitic steel, nickel-chrome-iron alloys and nickel-iron-chrome alloys. See NB-3683.2(b).
 $S_y =$ yield strength of the material at the Design Temperature, psi, taken from Table I-2.0.
 $\nu = 0.3 =$ Poisson's ratio.

(c) *Connecting Welds.* Connecting welds in accordance with the requirements of this Subsection are defined as either *flush* or *as-welded* welds.

(1) *Flush welds* are defined as those welds with contours as defined in the following sketch. The total thickness (both inside and outside) of the weld reinforcement shall not exceed $0.1t$. There shall be no concavity on either the interior or exterior surfaces and the finished contour shall nowhere have a slope greater than 7 deg., where the angle is measured from a tangent to the surface of the pipe, or on the tapered transition side of the weld, to the nominal transition surface.



(2) *As-welded welds* are defined as welds not meeting the special requirements of flush welds.

(d) *Loadings*. Loadings for which stress indices are given include internal pressure, bending and torsional moments, and temperature differences. The indices are intended to be sufficiently conservative to also account for the effects of transverse shear forces normally encountered in flexible piping systems. If, however, thrust or shear forces account for a significant portion of the loading on a given piping product, the effect of these forces shall be included in the design analysis. The values of the moments and forces shall be obtained from an analysis of the piping system in accordance with NB-3672. Loading terms are defined as follows.

P = design pressure, psi.

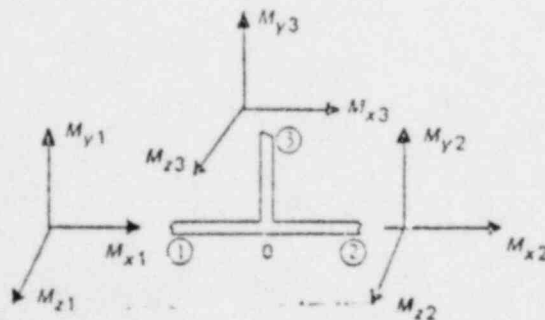
P_o = range of service pressure, psi.

P^* = the maximum value of pressure in the load cycle under consideration, psi.

M_1, M_2, M_3 = orthogonal moment loading components at a given position in a piping system, in.-lb.

$M_t = \sqrt{M_1^2 + M_2^2 + M_3^2}$ = resultant moment loading applied during the specified operating cycle for straight through products such as straight pipe, curved pipe or elbows, and concentric reducers.

$M_{i,j}$ = orthogonal moment components of a tee or branch connection as shown in the following sketch where $i = x, y, z$ and $j = 1, 2, 3$.



The moment components M_{x1} , M_{x2} , M_{y1} , M_{y2} , M_{z1} , and M_{z2} for the run are calculated at the intersection of the run and branch centerlines. The moment components M_{x3} , M_{y3} , and M_{z3} for a branch connection, where $d_o/D_o \leq 0.5$ may be calculated for a point on the branch center line at a distance $D_o/2$ from the intersection of the run and branch centerlines. Otherwise M_{x3} , M_{y3} , and M_{z3} are calculated at the intersection of the run and branch centerlines.

M_{xr} , M_{yr} , M_{zr} = run moment components for use with the stress indices of NB-3683.8 and NB-3683.9. Their numerical values are calculated as follows. If M_{i1} and M_{i2} , where $i = x, y, z$ have the same algebraic sign (+ or -), then $M_{ir} = 0$. If M_{i1} and M_{i2} have opposite algebraic signs, then M_{ir} equals the smaller of M_{i1} or M_{i2} . If M_{i1} and M_{i2} are unsigned, then M_{ir} may be taken as the smaller of M_{i1} or M_{i2} . Combination of signed and unsigned moments from different load sources shall be done after determination of

M_{ir}
 $M_b = \sqrt{M_{x3}^2 + M_{y3}^2 + M_{z3}^2}$ = resultant moment on the branch for branch connections or tees, in.-lb.

M_b^* = same as M_b except it includes only moments due to thermal expansion and thermal anchor movements.

$M_r = \sqrt{M_{xr}^2 + M_{yr}^2 + M_{z3}^2}$ = resultant moment on the run for branch connections or tees, in.-lb.

M_r^* = same as M_r except it includes only moments due to thermal expansion and thermal anchor movements.

For branch connections or tees the pressure term of Eqs. (9), (10), (11), and (13) shall be replaced by the following.

For Eq. (9):

$$B_1 \frac{P D_o}{2 T_r}$$

For Eqs. (10) and (13):

$$C_1 \frac{P_o D_o}{2 T_r}$$

For Eq. (11):

$$K_1 C_1 \frac{P_o D_o}{2 T_r}$$

For branch connections or tees, the moment term of Eqs. (9), (10), (11), (12), and (13) shall be replaced by the following pairs of terms:

For Eq. (9):

$$B_{2b} \frac{M_b}{Z_b} + B_{2r} \frac{M_r}{Z_r}$$

For Eqs. (10) and (13):

$$C_{2b} \frac{M_b}{Z_b} + C_{2r} \frac{M_r}{Z_r}$$

For Eq. (11):

$$C_{2b} K_{2b} \frac{M_b}{Z_b} + C_{2r} K_{2r} \frac{M_r}{Z_r}$$

For Eq. (12):

$$C_{2b} \frac{M_b^*}{Z_b} + C_{2r} \frac{M_r^*}{Z_r}$$

where the approximate section moduli are:

$$Z_b = \pi (r_m^*)^2 T_b^*$$

$$Z_r = \pi (R_m^2) T_r$$

NB-3683.2 Applicability of Indices - General. The B , C , and K stress indices given herein and in Table NB-3681(a)-1 predict stresses at a weld joint or within the body of a particular product. The stress indices given for ANSI B16.9, ANSI B16.28, MSS SP 48, and MSS SP 87 piping products apply only to seamless products with no connections, attachments, or other extraneous stress raiser on the body thereof. The stress indices for welds are not applicable if the radial weld shrinkage Δ is greater than $0.25t$.

For products with longitudinal butt welds the K_1 , K_2 , and K_3 indices shown shall be multiplied by 1.1 for *flush* welds or by 1.3 for *as-welded* welds. At the intersection of a longitudinal butt weld in straight pipe with a girth butt weld or girth fillet weld, the C_1 , K_1 , C_2 , K_2 , and K_3 indices shall be taken as the product of the respective indices.

(a) *Abutting Products.* In general and unless otherwise specified it is not required to take the product of stress indices for two piping products, such as a tee and a reducer when welded together, or a tee and a girth butt weld. The piping product and the weld shall be qualified separately.

For curved pipe or butt welding elbows welded together or joined by a piece of straight pipe less than 1 pipe diameter long, the stress indices shall be taken as the product of the indices for the elbow or curved pipe and the indices for the girth butt weld, except for B_1 and C_3 which are exempted.

(b) *Out-of-Round Products.* The stress indices given in Table NB-3681(a)-1 are applicable for products and welds with out-of-roundness not greater than $0.08t$, where out-of-roundness is defined as $D_{max} - D_{min}$. For straight pipe, curved pipe, longitudinal butt welds in straight pipe, girth butt welds, NB-4250 transitions and 1:3 transitions not meeting this requirement, the stress indices shall be modified as specified below.

(1) If the cross section is out-of-round such that the cross section is approximately elliptical, an acceptable value of K_1 may be obtained by multiplying the K_1 values in Table NB-3681(a)-1 by the factor F_{1a} , where

$$F_{1a} = 1 + \frac{D_{max} - D_{min}}{t} \left[\frac{1.5}{1 + 0.455 \left(\frac{D_o}{t} \right)^3 \frac{P^*}{E}} \right],$$

where P^* is the maximum value of pressure in the load cycle under consideration.

(2) If $D_{max} - D_{min}$ is not greater than $0.08D_o$, an acceptable value of K_1 may be obtained by multiplying the K_1 values in Table NB-3681(a)-1 by the factor F_{1b} , where

$$F_{1b} = 1 + \frac{M S_y}{P D_o / 2t},$$

where $M = 2$ for ferritic steels and nonferrous materials except nickel-chrome-iron alloys and nickel-iron-chrome alloys

$M = 2.7$ for austenitic steel, nickel-chrome-iron alloys, and nickel-iron-chrome alloys.

NB-3683.3 Straight Pipe Remote from Welds. The stress indices given in Table NB-3681(a)-1 apply for straight pipe remote from welds or other discontinuities except as modified by NB-3683.2.

NB-3683.4 Connecting Welds. The stress indices given in Table NB-3681(a)-1 are applicable for longitudinal butt welds in straight pipe; girth butt welds joining items with identical nominal wall thicknesses; and girth fillet welds used to attach socket weld fittings, socket weld valves, slip-on flanges, or socket welding flanges, except as modified herein and by NB-3683.2.

(a) *Longitudinal Butt Welds.* The stress indices shown in Table NB-3681(a)-1 are applicable for longitudinal butt welds in straight pipe except as modified by NB-3683.2.

(b) *Girth Butt Welds.* The stress indices shown in Table NB-3681(a)-1, except as modified herein and in NB-3683.2 are applicable to girth butt welds between two items for which the wall thickness is between $0.875t$ and $1.1t$ for an axial distance of $\sqrt{D_0 t}$ from the welding ends. Girth welds may also exhibit a reduction in diameter due to shrinkage of the weld material during cooling. The indices are not applicable if Δ/t is greater than 0.25, where Δ is the radial shrinkage measured from the nominal outside surface.

For *as-welded* girth butt welds joining items with nominal wall thicknesses $t < 0.237$, the C_2 index shall be taken as:

$$C_2 = 1.0 + 3(\delta/t), \text{ but not greater than } 2.1.$$

(c) *Girth Fillet Welds.* The stress indices shown in Table NB-3681(a)-1 are applicable to girth fillet welds used to attach socket weld fittings, socket weld valves, slip-on flanges, or socket welding flanges except as modified in NB-3683.2.

NB-3683.5 Welded Transitions. The stress indices given in Table NB-3681(a)-1, **except** as modified herein and in NB-3683.2 are applicable for NB-4250 welded transitions as defined under NB-3683.5(a) and for 1:3 welded transition as defined under NB-3683.5(b). Girth butt welds may also exhibit a reduction in diameter due to shrinkage of the weld material during cooling. The indices are not applicable if Δ/t is greater than 0.25.

(a) *NB-4250 Transitions.* The stress indices given in Table NB-3681(a)-1, except as modified herein and in NB-3683.2 are applicable to girth butt welds between an item for which the wall thickness is between $0.875t$ and $1.1t$ for an axial distance of $\sqrt{D_o t}$ from the welding end and another item for which the welding end is within the envelope of Fig. NB-4250-1, but with inside and outside surfaces that do not slope in the same direction. For transitions meeting these requirements the C_1 , C_2 , and C_3 indices shall be taken as:

$$\begin{aligned} C_1 &= 0.5 + 0.33 (D_o/t)^{0.3} + 1.5 (\delta/t); \text{ but not greater than } 1.8, \\ C_2 &= 1.7 + 3.0 (\delta/t); \text{ but not greater than } 2.1, \\ C_3 &= 1.0 + 0.03 (D_o/t); \text{ but not greater than } 2.0. \end{aligned}$$

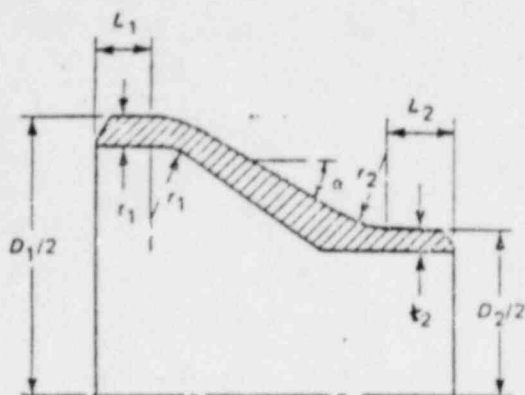
For *flush* welds and for *as-welded* joints between items with $t > 0.237$, δ may be assumed to be zero.

(b) *Transitions Within a 1:3 Slope.* The stress indices given in Table NB-3681(a)-1, except as modified herein and in NB-3683.2 are applicable to girth butt welds between an item for which the wall thickness is between $0.375t$ and $1.1t$ for an axial distance of $\sqrt{D_o t}$ from the welding end and another item for which the welding end is within an envelope defined by a 1:3 slope on the inside, outside, or both surfaces for an axial distance of $\sqrt{D_o t}$, but with inside and outside surfaces that do not slope in the same direction. For transitions meeting these requirements the C_1 , C_2 , and C_3 indices shall be taken as:

$$\begin{aligned} C_1 &= 1.0 + 1.5 (\delta/t); \text{ but not greater than } 1.8, \\ C_2 &= t_{max}/t + 3 (\delta/t); \text{ but not greater than the smaller of} \\ &\quad [1.33 + 0.04 \sqrt{D_o/t} + 3 (\delta/t)] \text{ or } 2.1, \\ C_3 &= 0.35 (t_{max}/t); \text{ but not greater than } 2.0, \end{aligned}$$

where t_{max} is the maximum wall thickness within the transition zone. If $(t_{max}/t) \leq 1.10$ the stress indices given in NB-3683.4(b) for girth butt welds may be used. For *flush* welds and for *as-welded* joints between items with $t > 0.237$, δ may be assumed to be zero.

NB-3683.6 Concentric Reducers. The stress indices given in Table NB-3681(a)-1, except as added to and modified herein and in NB-3683.2 are applicable to butt welding concentric reducers manufactured to the requirements of ANSI B16.9, MSS SP 48, or MSS SP 67 if the cone angle α , defined in the following sketch, is less than 60° ;



and if the wall thickness is not less than t_{1m} throughout the body of the reducer, except in and immediately adjacent to the cylindrical portion on the small end, where the thickness shall not be less than t_{2m} . The wall thicknesses t_{1m} and t_{2m} are the minimum thicknesses required to resist the design pressure P at the large end and small end, respectively, in accordance with Eq. (1), NB-3641.1.

(b) *Primary Plus Secondary Stress Indices.* The C_1 and C_2 stress indices given in (1) or (2) shall be used depending on the dimensions of the transition radii r_1 and r_2 .

- (1) For reducers with r_1 and $r_2 \geq 0.1 D_1$

$$C_1 = 1.0 + 0.0058 \alpha \sqrt{D_n/t_n}$$

$$C_2 = 1.0 + 0.36 \alpha^{0.4} (D_n/t_n)^{0.4} (D_2/D_1 - 0.5)$$

where D_n/t_n is the larger of D_1/t_1 and D_2/t_2 .

- (2) For reducers with r_1 and/or $r_2 < 0.1 D_1$

$$C_1 = 1.0 + 0.00465 \alpha^{1.285} (D_n/t_n)^{0.39}$$

$$C_2 = 1.0 + 0.0185 \alpha \sqrt{D_n/t_n}$$

where D_n/t_n is the larger of D_1/t_1 and D_2/t_2 .

(b) *Peak Stress Indices.* The K_1 and K_2 indices given in (1), (2), or (3) shall be used depending on the type of connecting weld, amount of mismatch, and thickness dimensions.

- (1) For reducers connected to pipe with flush girth butt welds:

$$K_1 = 1.1 - 0.1 \frac{L_m}{\sqrt{D_m t_m}}, \text{ but not less than } 1.0$$

$$K_2 = 1.1 - 0.1 \frac{L_m}{\sqrt{D_m t_m}}, \text{ but not less than } 1.0$$

where $L_m/\sqrt{D_m t_m}$ is the smaller of $L_1/\sqrt{D_1 t_1}$ and $L_2/\sqrt{D_2 t_2}$.

(2) For reducers connected to pipe with *as-welded* girth butt welds where $t_1, t_2 > 5/16$ in. and $\delta_1/t_1, \delta_2/t_2 \leq 0.1$:

$$K_1 = 1.2 - 0.2 \frac{L_m}{\sqrt{D_m t_m}}, \text{ but not less than } 1.0$$

$$K_2 = 1.8 - 0.8 \frac{L_m}{\sqrt{D_m t_m}}, \text{ but not less than } 1.0$$

where $L_m/\sqrt{D_m t_m}$ is the smaller of $L_1/\sqrt{D_1 t_1}$ and $L_2/\sqrt{D_2 t_2}$.

(3) For reducers connected to pipe with *as-welded* girth butt welds, where t_1 or $t_2 \leq 3/16$ in. or δ_1/t_1 or $\delta_2/t_2 > 0.1$:

$$K_1 = 1.2 - 0.2 \frac{L_m}{\sqrt{D_m t_m}}, \text{ but not less than } 1.0$$

$$K_2 = 2.5 - 1.5 \frac{L_m}{\sqrt{D_m t_m}}, \text{ but not less than } 1.0$$

where $L_m/\sqrt{D_m t_m}$ is the smaller of $L_1/\sqrt{D_1 t_1}$ and $L_2/\sqrt{D_2 t_2}$.

NB-3683.7 Curved Pipe or Butt-Welding Elbows. The stress indices given in Table NB-3681(a)-1, except as added to and modified herein and in NB-3683.2 are applicable to curved pipe or butt welding elbows manufactured to the requirements of ANSI B16.9, ANSI B16.28, MSS SP 48, or MSS SP 87.

(a) *Primary Stress Index.* The primary stress index B_2 for moment loadings shall be taken as:

$$B_2 = 1.30/h^{2/3}; \text{ but not less than } 1.0,$$

where

$$h = tR/r_m^2.$$

(b) *Primary Plus Secondary Stress Indices.* The C_1 and C_2 indices shall be taken as

$$C_1 = (2R - r_m)/2(R - r_m)$$

$$C_2 = 1.95/h^{2/3}; \text{ but not less than } 1.5,$$

where

$$h = tR/r_m^2.$$

NB-3683.8 Branch Connections per NB-3643. The stress indices given in Table NB-3681(a)-1, except as added to and modified herein and in NB-3683.2 are applicable to reinforced or unreinforced branch connections meeting the general requirements of NB-3643 and the additional requirements of NB-3683.8(a). Symbols are defined in NB-3683.1 and in Fig. NB-3643.3(a)-1.

(a) *Applicability.* The stress indices are applicable provided the following limitations are met.

(1) For branch connections in a pipe, the arc distance measured between the centers of adjacent branches along the outside surface of the run pipe is not less than three times the sum of the two adjacent branch inside radii in the longitudinal direction, or is not less than two times the sum of the two adjacent branch radii along the circumference of the run pipe.

(2) The axis of the branch connection is normal to the run pipe surface.

(3) The run pipe radius-to-thickness ratio $R_m/T_r < 50$; and the branch-to-run radius ratio $r'_m/R_m < 0.50$.

(4) The inside corner radius, r_1 [Fig. NB-3643.3(a)-1] for nominal pipe sizes greater than 4" ips shall be between 10% and 50% of T_r . The radius r_1 is not required for branch pipe sizes smaller than 4" ips.

(5) The branch-to-run fillet radius, r_2 , is not less than the larger of $T'_b/2$; $T_r/2$; or $(T'_b + y)/2$ [Fig. NB-3643.3(a)-1(c)].

(6) The branch-to-pipe fillet radius, r_3 , is not less than the larger of $0.002 \theta d_o$ or $2(\sin\theta)^3$ times offset [Fig. NB-3643.3(a)-1] where θ is expressed in degrees.

(7) If L_1 equals or exceeds $0.5\sqrt{r'_i T_b}$, then r'_m can be taken as the radius to the center of T_b .

(b) *Primary Stress Indices.* The primary stress indices B_{2b} and B_{2r} shall be taken as:

$$B_{2b} = 0.5 C_{2b}; \text{ but not less than } 1.0,$$

$$B_{2r} = 0.75 C_{2r}; \text{ but not less than } 1.0.$$

(c) *Primary Plus Secondary Stress Indices.* The C_1 , C_{2b} , and C_{2r} indices [for moment loadings see NB-3683.1(d)] shall be taken as:

$$C_1 = 1.4 \left(\frac{D_m}{T_r} \right)^{0.182} \left(\frac{d_m}{D_m} \right)^{0.367} \left(\frac{T_r}{t_n} \right)^{0.382} \left(\frac{t_n}{r_2} \right)^{0.148} \quad ; \text{ but not less than 1.2.}$$

If $r_2/t_n > 12$, use $r_2/t_n = 12$ for computing C_1 .

$$C_{2b} = 3 \left(\frac{R_m}{T_r} \right)^{2/3} \left(\frac{r'_m}{R_m} \right)^{1/2} \left(\frac{T'_b}{T_r} \right) \left(\frac{r'_m}{r'_p} \right) \quad ; \text{ but not less than 1.5}$$

$$C_{2r} = 1.15 \left(\frac{r'_m}{t_n} \right)^{1/4} \quad ; \text{ but not less than 1.5,}$$

where, for Figs. NB-3643.3(a)-1(a) and (b):

$$\begin{aligned} t_n &= T_b \text{ if } L_1 \geq 0.5 (d_m T_b)^{1/2} \\ &= T'_b \text{ if } L_1 < 0.5 (d_m T_b)^{1/2} \end{aligned}$$

For Fig. NB-3643.3(a)-1(c)

$$\begin{aligned} t_n &= T'_b + (2/3)y \text{ if } \theta \leq 30^\circ \\ &= T'_b + 0.385 L_1 \text{ if } \theta > 30^\circ. \end{aligned}$$

For Fig. NB-3643.3(a)-1(d)

$$t_n = T'_b = T'_r.$$

(d) *Peak Stress Indices.* The peak stress indices K_{2b} and K_{2r} for moment loadings [see NB-3683.1(d)] shall be taken as:

$$\begin{aligned} K_{2b} &= 1.0, \\ K_{2r} &= 1.75, \end{aligned}$$

and $K_{2r} C_{2r}$ shall be a minimum of 2.65.

NB-3683.9 Butt-Welding Jees. The stress indices given in Table NB-3681(a)-1, except as added to and modified herein and in NB-3683.2 are applicable to butt-welding tees manufactured to the requirements of ANSI B16.9, MSS SP 48, or MSS SP 87.

(a) *Primary Stress Indices.* The primary stress indices B_{2b} and B_{2r} shall be taken as:

$$\begin{aligned} B_{2b} &= 0.4 (R_m/T_r)^{2/3}; \text{ but not less than 1.0,} \\ B_{2r} &= 0.5 (R_m/T_r)^{2/3}; \text{ but not less than 1.0.} \end{aligned}$$

(b) *Primary Plus Secondary Stress Indices.* The C_{2b} and C_{2r} stress indices for moment loadings [see NB-3683.1(d)] shall be taken as:

$$C_{2b} = 0.67 (R_m/T_r)^{2/3}; \text{ but not less than } 2.0,$$

$$C_{2r} = 0.67 (R_m/T_r)^{2/3}; \text{ but not less than } 2.0.$$

(c) *Peak Stress Indices.* The peak stress indices K_{2b} and K_{2r} for moment loadings [see NB- 3683.1(d)] shall be taken as:

$$K_{2b} = 1.0 ,$$

$$K_{2r} = 1.0.$$

Table NB-3681(a)-1
STRESS INDICES FOR USE WITH EQUATIONS IN NB-3650

Piping Products and Joints ^a	Applicable for $D_o/t \leq 100$ for C or K indices; $D_o/t \leq 50$ for B indices									See Note
	Internal Pressure ^b			Moment Loading ^b			Thermal Loading			
	B_1	C_1^c	K_1^c	B_2	C_2^c	K_2^c	C_3	C_3^c	K_3^c	
Straight pipe, remote from welds or other discontinuities	0.5	1.0	1.0	1.0	1.0	1.0	1.0	—	1.0	<i>d</i>
Longitudinal butt welds in straight pipe										
(a) Flush	0.5	1.0	1.1	1.0	1.0	1.1	1.0	—	1.1	<i>e</i>
(b) As-welded; $t > 3/16$ in.	0.5	1.1	1.2	1.0	1.2	1.3	1.0	—	1.2	<i>e</i>
(c) As-welded; $t \leq 3/16$ in.	0.5	1.4	2.5	1.0	1.2	1.3	1.0	—	1.2	<i>e</i>
Girth butt welds between nominally identical wall thickness items										
(a) Flush	0.5	1.0	1.1	1.0	1.0	1.1	0.60	0.60	1.1	<i>f</i>
(b) As-welded	0.5	1.0	1.2	1.0	1.0	1.8	0.60	0.50	1.7	<i>f</i>
Girth fillet weld to socket weld										
Fittings, socket weld valves, slip-on or socket welding flanges	0.75	1.8	3.0	1.5	2.1	2.0	2.0	1.0	3.0	<i>g</i>
NB-4250 transitions										
(a) Flush	0.5	Note	1.1	1.0	Note	1.1	Note	1.0	1.1	<i>h</i>
(b) As-welded	0.5	Note	1.2	1.0	Note	1.8	Note	1.0	1.7	<i>h</i>
Transitions within a 1:3 slope envelope										
(a) Flush	0.5	Note	1.1	1.0	Note	1.1	Note	0.60	1.1	<i>i</i>
(b) As-welded	0.5	Note	1.2	1.0	Note	1.8	Note	0.60	1.7	<i>i</i>
Butt welding concentric reducers per ANSI B16.9 or B16.28	1.0	Note	Note	1.0	Note	Note	1.0	0.5	1.0	<i>j</i>
Curved pipe or butt welding elbows	0.5	Note	1.0	Note	Note	1.0	1.0	0.5	1.0	<i>k</i>
Branch connections per NB-3643	0.5	Note	2.0	Note	Note	Note	1.8	1.0	1.7	<i>l</i>
Butt welding tees	0.5	1.5	4.0	Note	Note	Note	1.0	0.5	1.0	<i>m</i>

^aFor definitions, applicability, and specific restrictions, see NB-3683.

^bFor the calculation of pressure and moment loads and special instructions regarding Eqs. (9) through (13), see NB-3683.1(d).

^cFor special instructions regarding the use of these indices for welded products, intersecting welds, abutting products or out-of-round products, see NB-3683.2.

^dSee NB-3683.3 "Straight Pipe Remote from Welds."

^eSee NB-3683.4(a) "Longitudinal Butt Welds."

^fSee NB-3683.4(b) "Girth Butt Welds."

^gSee NB-3683.4(a) "Girth Fillet Welds."

^hSee NB-3683.5(a) "NB-4250 Transitions."

ⁱSee NB-3683.5(b) "Transitions Within a 1:3 Slope."

^jSee NB-3683.6 "Concentric Reducers."

^kSee NB-3683.7 "Curved Pipe or Butt Welding Elbows." See also NB-3683.2(a) and (b).

^lSee NB-3683.8 "Branch Connections per NB-3643." See also NB-3683.1(d).

^mSee NB-3683.9 "Butt Welding Tees." See also NB-3683.1(d).

lines be used, but if two or more reliefs are combined, the discharge piping shall be designed with sufficient flow area to prevent undue back pressure.

(e) When the umbrella or drip pan type of connection between the pressure relieving safety device and the discharge piping is used, the discharge piping shall be so designed as to prevent binding due to expansion movements and shall be so dimensioned as to prevent the possibility of blow back of the effluent. Individual discharge lines shall be used in this application. Drainage shall be provided to remove water collected above the safety valve seat.

(f) Discharge lines from pressure relieving safety devices within the scope of this Subsection shall be designed to facilitate drainage if there is any possibility that the effluent can contain liquid.

NB-3680 STRESS INDICES AND FLEXIBILITY FACTORS

NB-3681 Scope

W78 (a) There are two types of analyses allowed by the rules of this Subarticle. The applicable *B*, *C*, and *K* indices to be used with Eqs. (9), (10), and (11) of NB-3650 are given in Table NB-3681(a)-1. The applicable indices to be used with the detailed analysis of NB-3200 are given in NB-3685 and NB-3686.

(b) Methods of determining flexibility factors for some commonly used piping products are given in NB-3687.

(c) Values of stress indices are tabulated for commonly used piping products and joints. Unless specific data, which data shall be referenced in the Stress Report, exist that would warrant lower stress indices than those tabulated or higher flexibility factors than those calculated by the methods of NB-3687, the stress indices given shall be used as minimums and the flexibility factors shall be used as maximums.

(d) For piping products not covered by NB-3680, stress indices and flexibility factors shall be established by experimental analysis (Appendix II) or theoretical analysis. Such test data or theoretical analysis shall be included in the Stress Report.

NB-3682 Definitions of Stress Indices and Flexibility Factors

(a) The general definition of a stress index for mechanical loads is:

$$B, C, K \text{ or } i = \frac{\sigma}{S}$$

where

- σ = elastic stress due to load, *L*
- S* = nominal stress due to load, *L*

For *B* indices, σ represents the stress magnitude corresponding to a limit load. For *C* or *K* indices, σ represents the maximum stress intensity due to load, *L*. For *i* factors, σ represents the principal stress at a particular point, surface and direction due to load, *L*. The nominal stress, *S*, is defined in detail in the tables of stress indices.

(b) The general definition of a stress index for thermal loads is:

$$C, K = \frac{\sigma}{E\alpha\Delta T}$$

where

- σ = maximum stress intensity due to thermal difference, ΔT
- E* = modulus of elasticity
- α = coefficient of thermal expansion
- ΔT = thermal difference

The values of *E*, α and ΔT are defined in detail in NB-3650.

(c) Flexibility factors are identified herein by *k*, with appropriate subscripts. The general definition of a flexibility factor is:

$$k = \frac{\theta_{ab}}{\theta_{nom}}$$

where

- θ_{ab} = rotation of end *a*, with respect to end *b*, due to a moment load, *M*, and in the direction of the moment *M*
- θ_{nom} = nominal rotation due to moment load *M*

The flexibility factor *k* and nominal rotation θ_{nom} are defined in detail for specific components in NB-3687.

NB-3683 Stress Indices for Use With NB-3650

NB-3683.1 Definitions for Stress Indices	
<i>P</i> = Design Pressure, psi	For ANSI B16.9, ANSI B16.28 or MSS SP 48 piping products, these are dimensions of the equivalent pipe.
<i>D_o</i> = nominal outside diameter of pipe, in.	
<i>D_i</i> = nominal inside diameter of pipe, in.	
<i>t</i> = nominal wall thickness of pipe, in.	
<i>r</i> = 0.0491 (<i>D_o</i> - <i>D_i</i>), in. ⁴	

(a) For Tapered Transition Joints: Use dimensions of thin end of taper.

(b) For Reducing Branch Connections or Reducing Tees:

(1) Pressure dependent term: Use dimensions of run or branch, whichever gives larger value of D_o/t ;

(2) Moment loads: See Notes 5, 7, & 9 of Table NB-3683.2-1.

(c) For Reducers:

(1) Pressure dependent term: Use dimensions of large or small end, whichever gives the larger value of D_o/t ;

(2) Moment dependent term: Use dimensions of small end.

W78 NB-3683.2 B, C, and K Indices. Table NB-3681(a)-1 gives values of B, C, and K indices, along with additional dimensional definitions and dimensional restrictions.

NB-3684 Stress Indices for Detailed Analysis

NB-3684.1 Definition of Stress Components. The symbols for the stress components and their definitions are given in Fig. NB-3684.1-1. These definitions are applicable to all piping products, and the stress indices given in the tables in NB-3685 and NB-3686 are so defined.

335g

NB-3685 Curved Pipe or Welding Elbows

NB-3685.1 Applicability of Indices. The indices given in Tables NB-3685.1-1 and NB-3685.1-2 give stresses in curved pipe or elbows at points remote from girth or longitudinal welds or other local discontinuities. Stresses in elbows with local discontinuities such as longitudinal welds, support lugs, and branch connections in the elbow shall be obtained by appropriate theoretical analysis or by experimental analysis in accordance with Appendix II.

NB-3685.2 Nomenclature (Fig. NB-3685.2-1)

- P = internal pressure, psi
- D_o = nominal outside diameter of cross section, in.
- $D_i = D_o - 2(t_m + A)$, in.
- t_m = minimum specified wall thickness, in.
- A = an additional thickness, in. (NB-3641.1)
- R = bend radius, in.
- r = mean cross section radius, in.
- $\lambda = t_m R / r^2 \sqrt{1 - v^2}$ (Table NB-3685.1-2 limited to $\lambda \geq 0.2$)

$D_1(D_2)$ = maximum (minimum) outside diameter of elbow with out of round cross section essentially describable as an ellipse or oval shape (Fig. NB-3685.2-1), in.

Z = section modulus of cross section = $0.0982 (D_o^4 - D_i^4) / D_o$, in.³

E = modulus of elasticity, psi (Table I-5.0)

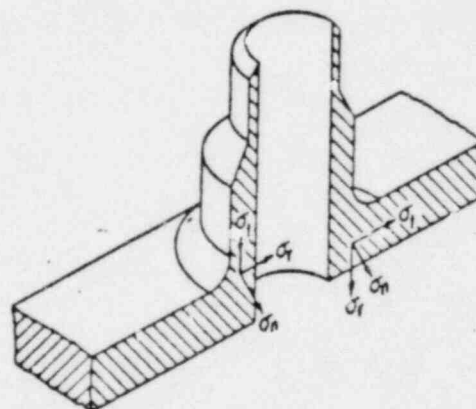
NB-3685.3 Stress From Stress Indices. To obtain stresses from stress index:

Load	Multiply Stress Index by:
Internal Pressure	P
M_x	$M_x / 2Z$
M_y	M_y / Z
M_z	M_z / Z

NB-3685.4 Classification of Stresses. For analysis of a curved pipe or welding elbow to NB-3210, the following rules shall apply to the classification of stresses developed under a load controlled in-plane or out-of-plane moment as distinguished from a displacement controlled loading.

(a) The entire membrane portion of the axial, circumferential, and torsional stresses shall be considered as primary (P_L).

(b) Seventy-five percent (75%) of the through-wall bending stresses in both the axial and the circumfer-



- σ_r = the stress component in the plane of the section under consideration and parallel to the boundary of the section
- σ_n = the stress component normal to the plane of the section
- σ_t = the stress component normal to the boundary of the section
- σ = the stress intensity (combined stress) at the point under consideration

FIG. NB-3684.1-1 DIRECTION OF STRESS COMPONENTS

W78
S79
W79

TABLE NB-3691(a)-1
STRESS INDICES FOR USE WITH EQUATIONS IN NB-3650

(Not Applicable for $D_o/t > 100$)

Piping Products and Joints	Internal Pressure			Moment Loading ^a			Thermal Loading		
	B ₁	C ₁	K ₁	B ₂	C ₂	K ₂	C ₃	C' ₃	K ₃
Straight pipe, remote from welds or other discontinuities	0.5	1.0	1.0 ¹	1.0	1.0	1.0	1.0	...	1.0
Girth butt weld between straight pipe or between pipe and butt welding components ^{2,12}									
(a) flush	0.5	1.0	1.1 ¹	1.0	1.0	1.1	1.0	0.5	1.1
(b) as welded $t > 3/16$ in. [and $\delta/t \leq 0.1$]	0.5	1.1	1.2 ¹	1.0	1.0	1.8	1.0	0.5	1.7
(c) as welded $t \leq 3/16$ in. [or $\delta/t > 0.1$]	0.5	1.1	1.2 ¹	1.0	1.4	2.5	1.0	0.5	1.7
Girth fillet weld to socket weld fittings or socket welding flanges	0.75	2.0	3.0	1.5	2.1	2.0	1.8	1.0	3.0
Longitudinal butt welds in straight pipe									
(a) flush	0.5	1.0	1.1 ¹	1.0	1.0	1.1	1.0	...	1.1
(b) as welded $t > 3/16$ in.	0.5	1.1	1.2 ¹	1.0	1.2	1.3	1.0	...	1.2
(c) as welded $t \leq 3/16$ in.	0.5	1.4	2.5 ¹	1.0	1.2	1.3	1.0	...	1.2
Tapered transition joints per NB-4225 and Fig. NB-4223-1 ^{4,12}									
(a) flush or no girth weld closer than \sqrt{rt}	0.5	*	1.2	1.0	*	1.1	*	1.0	1.1
(b) as welded	0.5	*	1.2	1.0	*	1.8	*	1.0	1.7
Branch connections per NB-3643 ^{2,11}	0.5	1.5	2.2	?	?	?	1.8	1.0	1.7
Curved pipe or butt welding elbows per ANSI B16.9, ANSI B16.28, MSS SP-87, or MSS SP-48 ^{10,11}	0.5	$(2R-r)\sqrt{2} \times (R-r)$ [Note (4)]		*	*	1.0	1.0	0.5	1.0
Butt welding tees per ANSI B16.9, MSS SP-87, or MSS SP-48 ^{10,11}	0.5	1.5	4.0	*	*	1.0	1.0	0.5	1.0
Butt welding reducers per ANSI B16.9, MSS SP-87, or MSS SP-48 ^{10,11}	1.0	¹²	¹⁴	1.0	¹²	¹⁴	1.0	0.5	1.0

NOTES:

(1) (a) The values of K_1 shown for these components are applicable for components with out of roundness not greater than $0.08t$, where out of roundness is defined as $D_{max} - D_{min}$, and

D_{max} = maximum outside diameter of cross section, in.
 D_{min} = minimum outside diameter of cross section, in.
 t = nominal wall thickness, in.

(b) If the cross section is out of round such that the cross section is approximately elliptical, an acceptable value of K_1 may be obtained by multiplying the tabulated values of K_1 by the factor F_{1a} :

$$F_{1a} = 1 + \frac{D_{max} - D_{min}}{t} \left[\frac{1.5}{1 + 0.455 \left(\frac{D_o}{t} \right)^3 \frac{P}{E}} \right]$$

where D_o = nominal outside diameter, in.
 P = internal pressure, psi
 (use maximum value of pressure in the load cycle under consideration)
 E = modulus of elasticity of material at room temperature, psi

Other symbols are defined in (2).

(c) If $D_{max} - D_{min}$ is not greater than $0.08 D_o$, and acceptable value of K_1 may be obtained by multiplying the tabulated values of K_1 by the factor F_{1b} :

$$F_{1b} = 1 + \frac{MS_y}{P D_o / 2t}$$

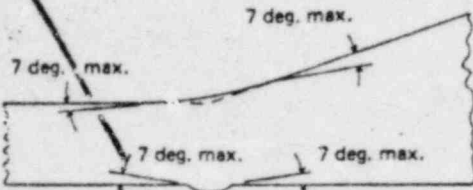
where $M = 2$ for ferritic steels and nonferrous materials except nickel-chrome-iron alloys and nickel-iron-chrome alloys
 $M = 2.7$ for austenitic steels, nickel-chromium-iron alloys, and nickel-iron-chromium alloys;
 S_y = yield strength at design temperature, psi (Tables I-2.0)
 P = Design Pressure, psi
 D_o and t are defined in (a) and (b).

(2) Welds in accordance with the requirements of this Subsection.

(a) Flush welds are defined as those welds with contours as defined in the following sketch. Thickness of weld reinforcement (total inside and outside) shall not exceed $0.1t$. There shall be no concavity on either the interior or exterior surfaces. The finished contour shall nowhere have a slope (angle measured $1 \mu m$ tangent to surface of

W78

pipe or, on tapered transition side of weld, to the nominal transition surface) greater than 7 deg., see sketch below.



(b) *As-welded* is defined as welds not meeting the special requirements for *flush welds*. At the intersection of a longitudinal butt weld in straight pipe with a girth butt weld or girth fillet weld.

$$B_1 = 0.5 \text{ and } B_2 = 1.0$$

The C_1 , K_1 , C_2 , K_2 , and K_3 indices shall be the product of the respective indices for the longitudinal weld and girth weld. For example, at the intersection of an *as-welded* girth butt weld with an *as-welded* longitudinal butt weld, C_1 is $1.1 \times 1.1 = 1.21$. C_2 for a girth fillet weld intersecting a longitudinal weld shall be taken as 2.0.

(3) The stress indices given are applicable only to branch connections in straight pipe with branch axis normal to the pipe surface and which meet the dimensional requirements and limitations of NB-3686 and Fig. NB-3686.1-1.

(4) R = curved pipe or elbow radius, in.
 r = mean radius of cross section, in.
 $t = (D_o - t)/2$, where t = nominal wall thickness

W78 (5) The values of the moment, M_T , shall be obtained from an analysis of the piping system in accordance with NB-3672. M_T is defined as the range of moment loading applied during the specified operating cycle.

Straight Through Pipe

$$M_t = \text{moment at Point A}$$

$$M_t = \sqrt{M_1^2 + M_2^2 + M_3^2}$$

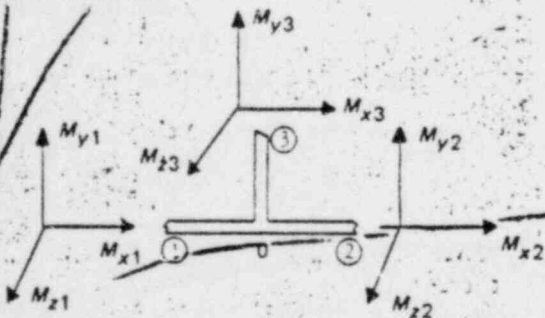
Curved Pipe or Welding Elbow

$$M_t = \text{moment at Point A}$$

$$M_t = \sqrt{M_1^2 + M_2^2 + M_3^2}$$

Branch Pipe

Moments calculated for point at intersection of run and branch center lines



For M_b

$$M_b = \sqrt{M^2_{x3} + M^2_{y3} + M^2_{z3}} = \text{resultant moment on branch}$$

For M_r

$$M_r = \sqrt{M^2_{xr} + M^2_{yr} + M^2_{zr}} = \text{resultant moment on run}$$

where M_{xr} , M_{yr} and M_{zr} are determined as follows:

If M_{i1} and M_{i2} have the same algebraic sign, then $M_{ir} = 0$. If M_{i1} and M_{i2} have different algebraic signs, then M_{ir} is the smaller of M_{i1} or M_{i2} where $i = x, y, z$

For branch connections of tees, the M_i term of Equations (9), (10), (11), or (12), shall be replaced by the following pairs of terms:

Equation (9) $B_{1b} \frac{M_b}{Z_b} + B_{1r} \frac{M_r}{Z_r}$

Equations (10) & (12) $C_{1b} \frac{M_b}{Z_b} + C_{1r} \frac{M_r}{Z_r}$

Equation (11) $C_{1b} K_{1b} \frac{M_b}{Z_b} + C_{1r} K_{1r} \frac{M_r}{Z_r}$

where

$$Z_b = \pi (r'_m)^2 T_b$$

$$Z_r = \pi R_m^2 T_r$$

For branch connections per NB-3643 see Note (3) above
 r'_m , T_b , R_m , and T_r are defined in Fig. NB-3686.1-1
 For butt welding tees per ANSI B16.9, MSS SP-87, or MSS SP-48:

- r'_m = mean radius of designated branch pipe
- T_b = nominal wall thickness of designated branch pipe
- R_m = mean radius of designated run pipe
- T_r = nominal wall thickness of designated run pipe

(6) Indices are applicable to tapered transition joints with a girth butt weld at the thin end of the transition.

$$C_1 = 1.3 + 0.003 (D_o/t) + 1.5 (b/t) \text{ but not greater than } 2.0$$

$$C_2 = 1.4 + 0.004 (D_o/t) + 3.0 (b/t) \text{ but not greater than } 2.1$$

$$C_3 = 1.2 + 0.008 (D_o/t)$$

(7) $B_{2b} = 0.50 C_{2b}$, but not less than 1.0
 $B_{2r} = 0.75 C_{2r}$, but not less than 1.0
 $C_{2b} = 3 (R_m/T_r)^{2/3} (r'_m/R_m)^{1/2} (T_b/T_r) (r'_m/r_p)$, but not less than 1.5. (R_m , T_r , r'_m , T_b and r_p are defined in Fig. NB-3686.1-1.)

$$K_{2b} = 1.0$$

$$K_{2r} = 0.8 (R_m/T_r)^{2/3} (r'_m/R_m)$$
, but not less than 2.0
 $K_{2r} = 2.0$

The product of $C_{2r} K_{2r}$ shall be a minimum of 3.0.

(8) $C_2 = 1.95/b_2^{2/3}$, but not less than 1.5
 $B_2 = 0.75 C_2$
 $b_2 = tR/r^2$, where t = nominal pipe wall thickness; R = bend radius of curved pipe or elbow; r = mean pipe radius, $(D_o - t)/2$

S79 (9) $B_{1a} = 0.40(R_m/T)^{2/3}$, but not less than 1.0
 $B_{2a} = 0.75(R_m/T)^{2/3}$, but not less than 1.0
 $C_{2a} = C_{2r} = 0.67(R_m/T)^{2/3}$, but not less than 2.0, where
 R_m = mean radius of designated run pipe;
 T = nominal wall thickness of designated run pipe
 $K_{1a} = K_{2r} = 1.0$

(c) Reducers in which r_1 and $r_2 \geq 0.1D$,

$$C_1 = 1 + 0.0058\alpha\sqrt{D_n/t_n}$$

$$C_2 = 1 + 0.36\alpha^{2.4}(D_n/t_n)^{0.4}(D_1/D_2)^{-0.5}$$

where D_n/t_n is the larger of D_1/t_1 and D_2/t_2 .

(d) Reducers in which r_1 and/or $r_2 < 0.1D$,

$$C_1 = 1 + 0.00465\alpha^{1.25}(D_n/t_n)^{0.18}$$

$$C_2 = 1 + 0.0185\alpha\sqrt{D_n/t_n}$$

where D_n/t_n is the larger of D_1/t_1 and D_2/t_2 .

(14) The K indices given in (a), (b), and (c) apply for reducers attached to the connecting pipe with flush or as-welded girth welds as defined in footnote (2). Note that the connecting girth weld must also be checked separately for compliance.

(a) For reducers connected to pipe with flush girth butt welds:

$$K_1 = 1.1 - 0.1 \frac{L_m}{\sqrt{D_m t_m}}, \text{ but not less than } 1.0$$

$$K_2 = 1.1 - 0.1 \frac{L_m}{\sqrt{D_m t_m}}, \text{ but not less than } 1.0$$

where $L_m/\sqrt{D_m t_m}$ is the smaller of $L_1/\sqrt{D_1 t_1}$ and $L_2/\sqrt{D_2 t_2}$.

(b) For reducers connected to pipe with as-welded girth butt welds where $r_1, r_2 > 3/16$ in. and $\delta_1/t_1, \delta_2/t_2 < 0.1$:

$$K_1 = 1.2 - 0.2 \frac{L_m}{\sqrt{D_m t_m}}, \text{ but not less than } 1.0$$

$$K_2 = 1.8 - 0.8 \frac{L_m}{\sqrt{D_m t_m}}, \text{ but not less than } 1.0$$

where $L_m/\sqrt{D_m t_m}$ is the smaller of $L_1/\sqrt{D_1 t_1}$ and $L_2/\sqrt{D_2 t_2}$.

(c) For reducers connected to pipe with as-welded girth butt welds, where r_1 or $r_2 \leq 3/16$ in. or δ_1/t_1 or $\delta_2/t_2 > 0.1$:

$$K_1 = 1.2 - 0.2 \frac{L_m}{\sqrt{D_m t_m}}, \text{ but not less than } 1.0$$

$$K_2 = 2.5 - 1.5 \frac{L_m}{\sqrt{D_m t_m}}, \text{ but not less than } 1.0$$

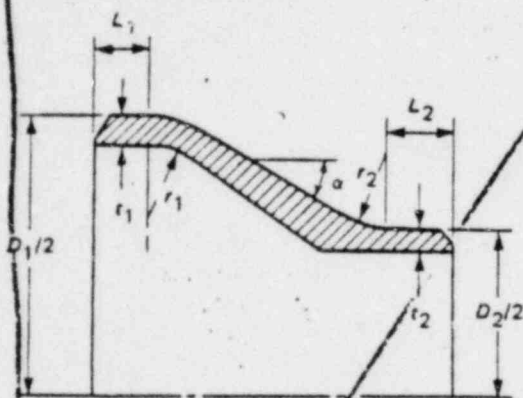
where $L_m/\sqrt{D_m t_m}$ is the smaller of $L_1/\sqrt{D_1 t_1}$ and $L_2/\sqrt{D_2 t_2}$.

W78 (10) The K indices given for fittings per ANSI B16.9, ANSI B16.28, MSS SP-87, or MSS SP-48 apply only to seamless fittings with no connections, attachments, or other extraneous stress raisers on the bodies thereof. For fittings with longitudinal butt welds, the K indices shown shall be multiplied by 1.1, for flush welds as defined in Note (2); by 1.3 for welds not meeting the requirements for flush welds.

(11) The stress indices given predict stresses which occur in the body of a fitting. It is not required to take the product of stress indices for two piping products such as a tee and a reducer, or a tee and a girth butt weld when welded together except for the case of curved pipe or butt welding elbows welded together or joined by a piece of straight pipe the length of which is less than 1 pipe diameter. For this specific case the stress index for the curved pipe or butt welding elbow must be multiplied by that for the girth butt weld. Excluded from this multiplication are the B_1 and C_1 indices. Their value is to be: $B_1 = 1.0$, $C_1 = 0.50$.

(12) δ is defined as the maximum permissible mismatch as shown in Fig. NB-4233-1. A value of δ less than 3/32 in. may be used provided the smaller mismatch is specified for fabrication. For flush welds, defined in footnote (2), δ may be taken as zero.

(13) (a) Nomenclature



t_1 = nominal wall thickness, large end
 t_2 = nominal wall thickness, small end
 D_1 = nominal outside diameter, large end
 D_2 = nominal outside diameter, small end
 α = cone angle, deg.

(b) The indices given in (c) and (d) apply if the following conditions are met.

(1) Cone angle, α does not exceed 60 deg. and the reducer is concentric.

(2) The wall thickness is not less than $t_{1,m}$ throughout the body of the reducer, except in and immediately adjacent to the cylindrical portion on the small end, where the thickness shall not be less than $t_{2,m}$. Wall thicknesses $t_{1,m}$ and $t_{2,m}$ are to be obtained by Equation (1), NB-3641.1.

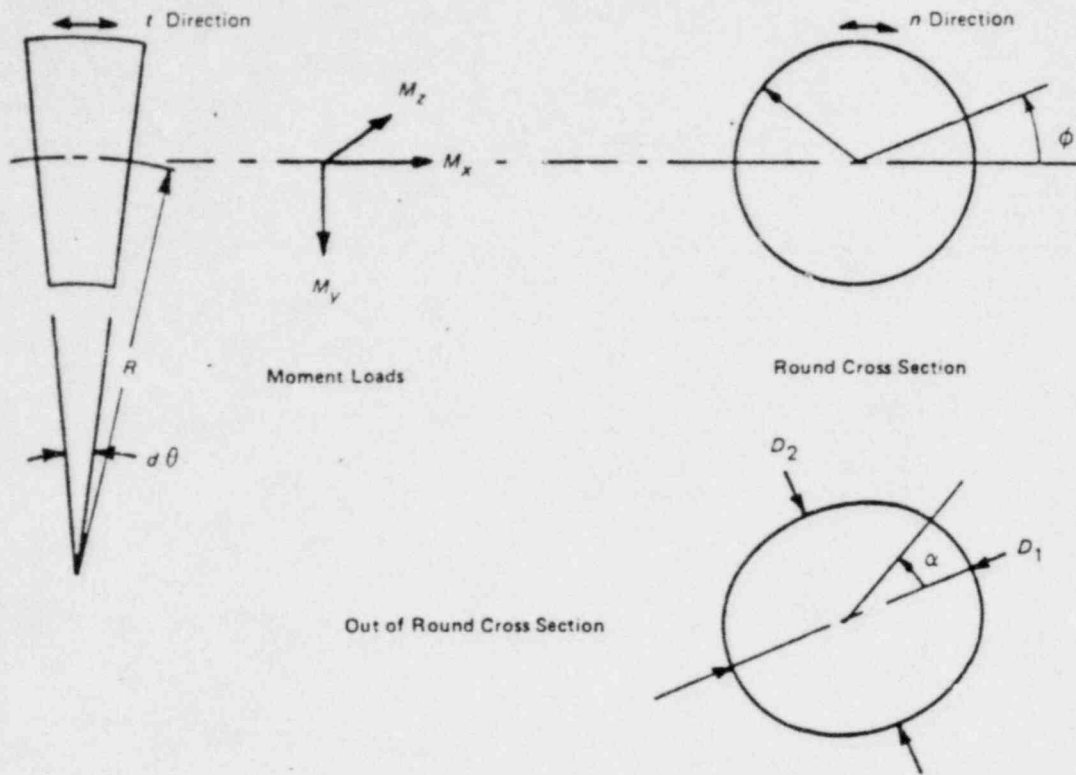


FIG. NB-3685.2-1 NOMENCLATURE ILLUSTRATION FOR ELBOWS

ential directions shall be classified as primary (P_b). The remaining 25% shall be classified as secondary (Q).

The stresses induced by displacement controlled in-plane or out-of-plane moments shall be classified as secondary (Q).

NB-3686 Branch Connections With Branch/Run Diameter Ratio Not Over One-Half

NB-3686.1 Applicability of Indices. The indices given in Table NB-3686.1-1 apply if the conditions in (a) through (h) are met.

(a) The reinforcing area requirements of NB-3643 are met.

(b) The axis of the branch pipe is normal to the surface of the run pipe wall.²²

²²If the axis of the branch pipe makes an angle, ϕ , with the normal to the run pipe wall, an estimate of the σ_n index on the inside may be obtained from the following equations, provided $d/D \leq 0.15$:

For lateral connections in pipe:

$$i_2 = i_1 [1 + (\tan \phi)^2]^{1.33}$$

(c) For branch connections in a pipe, the arc distance measured between the centers of adjacent branches along the surface of the run pipe is not less than three times the sum of their inside radii in the longitudinal direction or is not less than two times the sum of their radii along the circumference of the run pipe.

(d) For branch connections in a formed head, the arc distance measured between the centers of adjacent branches along the surface of the head is not less than three times the sum of their inside radii. The radius of curvature of the formed head is essentially constant and equal to R_h for a distance of $(r_m + \sqrt{R_h T_h})$ measured along the surface of the formed head from the center of the branch connection.

For hillside connections in pipe:

$$i_2 = i_1 [1 + 2(\sin \phi)^2]$$

where

- i_1 = the σ_n inside stress index of Table NB-3686.1-1 for a radial connection
- i_2 = the estimated σ_n inside stress index for the nonradial connection

TABLE NB-3686.1-1
BRANCH CONNECTIONS WITH RESTRICTIONS
GIVEN IN NB-3686, INTERNAL PRESSURE

(a) Branch Connections in Pipe Stress Index, <i>i</i>				
Stress	Longitudinal Plane		Transverse Plane	
	Inside	Outside	Inside	Outside
σ_n	3.1	1.2	2.0	2.1
σ_t	-0.2	1.0	-0.2	2.6
σ_r	$-t_r/R_r$	0	$-t_r/R_r$	0
σ	3.3	1.2	1.2	2.6

(b) Branch Connections in Formed Heads Stress Index, <i>i</i>		
Stress	Inside Corner	Outside Corner
σ_n	2.0	2.0
σ_t	-0.2	2.0
σ_r	$-2t_h/R_h$	0
σ	2.2	2.0

(e) Dimensional ratios are limited as follows:

Branch Connections in Pipe	Branch Connections in Formed Heads
$\frac{R_m}{T_r} \leq 50$	$\frac{R_{fh}}{T_h} \leq 50$
$\frac{r'_m}{R_m} \leq 0.5$	$\frac{r'_m}{R_{fh}} \leq 0.5$

(f) The inside corner radius, r_1 (Fig. NB-3686.1-1), is between 10% and 50% of T_r .

(g) The outer radius, r_2 (Fig. NB-3686.1-1) is not less than the larger of $T'_b/2$ ($T'_b + y$)/2 [Fig. NB-3686.1-1(c)] or $T_r/2$.

(h) The outer radius, r_3 (Fig. NB-3686.1-1), is not less than the larger of

- (1) $0.002 \theta d_o$
- (2) $2(\sin \theta)^2$ times the offset, for the configurations shown in Figs. NB-3686.1-1(a) and NB-3686.1-1(b).

NB-3686.2 Nomenclature (Fig. NB-3686.1-1)

- r = inside radius of branch pipe, in.
- r' = mean radius of branch pipe, in.
- T'_b = nominal thickness of branch pipe, in.
- R_m = mean radius of run pipe, in.
- R_h = mean radius of formed head in the vicinity of the branch connection, in.
- T_r = nominal thickness of run pipe, in.

- T_h = nominal thickness of formed head, in.
- $T_r = \begin{cases} T_r & \text{for branch connection in pipe, in.} \\ T_h & \text{for branch connection in formed head, in.} \end{cases}$
- d_o = outside diameter of branch, in.
- $T_b, \theta, r_1, r_2, r_3, r_p,$ and y are defined in Fig. NB-3686.1-1
- t_r = minimum required thickness of run pipe, calculated as a plain cylinder
- t_h = minimum required thickness of formed head, calculated as a spherical shell of inside radius, R_h
- P = internal pressure, psi
- $\sigma_n, \sigma_t, \sigma_r,$ are stresses as defined in NB-3680, psi
- σ = stress intensity, psi

NB-3686.3 Stresses from Stress Indices

(a) For branch connections in pipe, multiply stress indices by:

$$\frac{PR_r}{t_m}$$

(b) For branch connections in formed heads, multiply stress indices by:

$$\frac{PR_h}{2t_h}$$

NB-3687 Flexibility Factors

NB-3687.1 Straight Pipe

$k = 1.0 \quad \theta_{nom} = \frac{Ml}{EI}$

for $M = M_1$ or M_2

$k = 1.0 \quad \theta_{nom} = \frac{Ml}{GJ}$

for $M = M_3$

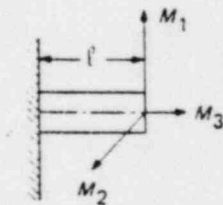
l = one pipe diameter

I = plane moment of inertia, in.⁴

J = polar moment of inertia, in.⁴

E = modulus of elasticity, psi

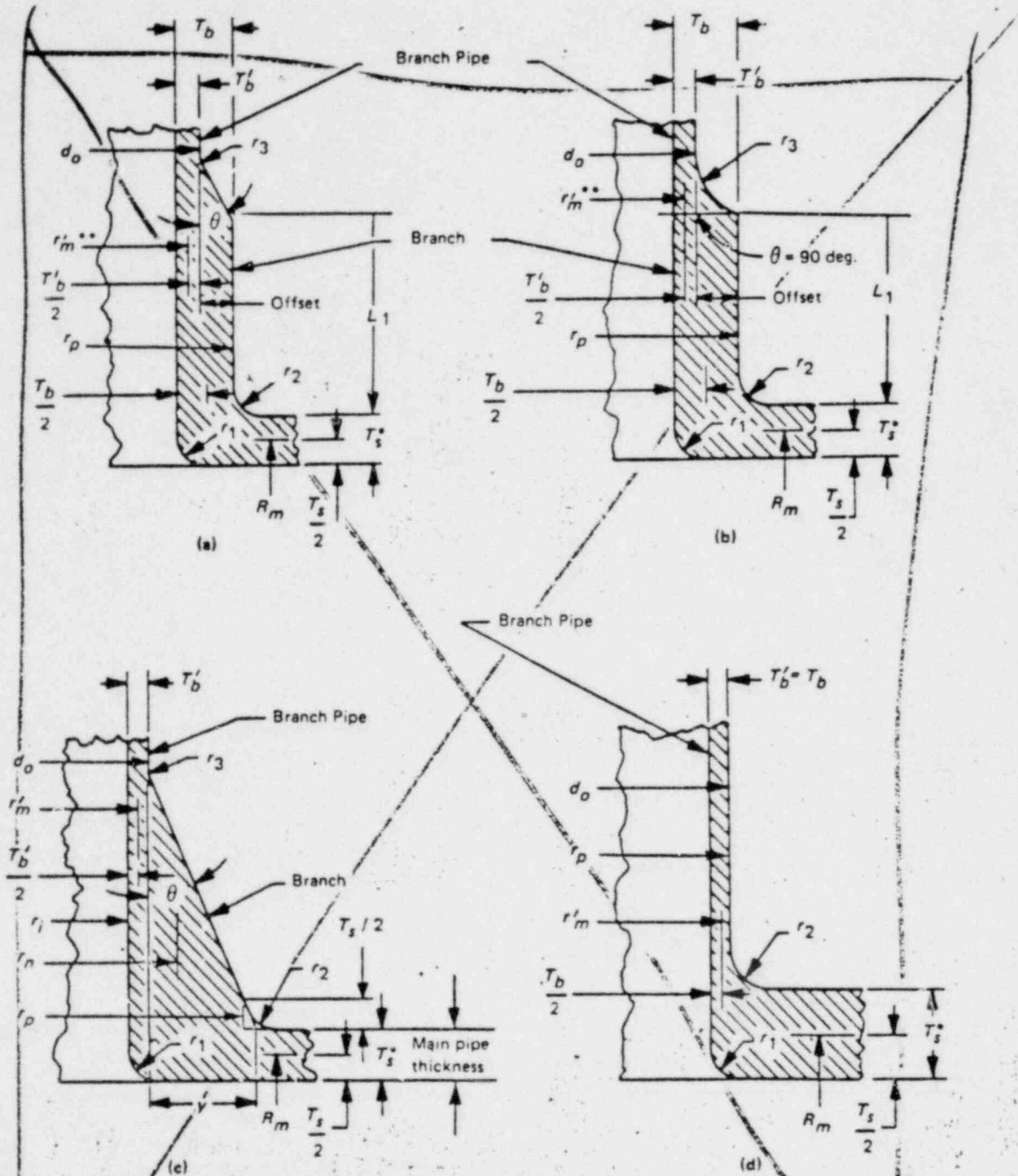
G = shear modulus, psi



NB-3687.2 Curved Pipe and Welding Elbows. The flexibility factors may be calculated by the equations given below for k , provided²³ that:

- (a) R/r is not less than 1.7;
- (b) Center line length ($R\alpha$) is greater than $2r$;
- (c) There are no flanges or other similar stiffeners

²³The flexibility of a curved pipe or welding elbow is reduced by end effects, provided either by the adjacent straight pipe or by the proximity of other relatively stiff members which inhibit ovalization of the cross section. In certain cases, these end effects may also reduce the stress. Additional work is underway to provide guidance for both flexibility factors and stress indices where end effects are significant.



*NOTE: $T_s = T_r$ for branch connection in pipe
 $T_s = T_h$ for branch connection in formed head

**NOTE: If L_1 equals or exceeds $0.5 \sqrt{r_1 T_b}$ then r'_m can be taken as the radius to the center of T_b .

FIG. NB-3686.1-1 NOZZLE DIMENSIONS

W78

within a distance r from either end of the curved section of pipe or from the ends of welding elbows.

For M_1 or M_2 :

$$k = \frac{1.65}{h} \left(\frac{1}{1 + \frac{Pr}{tE} X_k} \right)$$

but not less than 1.0

$$\theta_{nom} = \frac{R}{EI} \int_0^\alpha M(d\alpha)$$

For M_3 :

$$k = 1.0$$

$$\theta_{nom} = \frac{R}{GJ} \int_0^\alpha M(d\alpha)$$

in both cases

$$h = tR/r^2$$

R = bend radius, in.

P = internal pressure, psi

r = pipe or elbow mean radius, in.

t = pipe or elbow nominal wall thickness, in.

$$X_k = 6(r/t)^{1/3} (R/r)^{1/3}$$

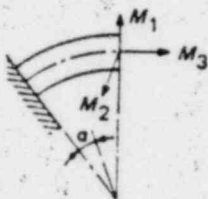
I = plane moment of inertia of cross section, in.⁴

J = polar moment of inertia of cross section, in.⁴

E = modulus of elasticity, psi

G = shear modulus of elasticity, psi

α = arc angle, radians



NB-3687.3 Miter Bends. The requirements of NB-3681(d) apply.

NB-3687.4 Welding Tee or Branch Connections. For welding tees (ANSI B16.9) or branch connections (NB-3643) not included in NB-3687.5, the load displacements relationships shall be obtained by assuming that the run pipe and branch pipe extend to the intersection of the run pipe center line with the branch pipe center line. The imaginary juncture is to be assumed rigid, and the imaginary length of branch pipe from the juncture to the run pipe surface is also to be assumed as rigid.

NB-3687.5 Branch Connection in Pipe Meeting the Requirements of NB-3640. For branch connections in piping meeting the requirements of NB-3640 and with branch diameter to run diameter ratio not over one-third, the requirements of (a) through (d) apply.

(a) The values of k are given below.

$$k = 0.09 \left(\frac{D}{T_c} \right)^{1/2} \left(\frac{T_b}{T_r} \right) \left(\frac{d}{D} \right) \text{ for } M_{23}$$

$$\theta_{nom} = \frac{Md}{EI_b}$$

$$k = 0.27 \left(\frac{D}{T_c} \right)^{1/2} \left(\frac{T_b}{T_r} \right) \left(\frac{d}{D} \right) \text{ for } M_{23}$$

where

$M = M_{23}$ or M_{33} , which are defined in footnote 5 of Table NB-3683.2-1, in. lb.

D = run pipe outside diameter, in.

d = branch pipe outside diameter, in.

T_r = run pipe nominal wall thickness, in.

T_b = branch pipe nominal wall thickness, in.

T_c = equivalent thickness, in.

NB-3683.1 (d)

(b) For branch connections per Fig. NB-3686-1 sketches (a), (b), and (d) and extruded outlets per NB-3643

$$T_c = T_r$$

NB-3643.3(a)-1

(c) For branch connections per Fig. NB-3686-1 sketch (c)

$$T_c = T_r + \frac{A}{d} \text{ for } M_{23}$$

$$T_c = T_r + \frac{A}{2d} \text{ for } M_{33}$$

where

A = actual area of reinforcing within the zone of reinforcement given in NB-3643.3(b), sq in.

I_b = moment of inertia of branch pipe, in.⁴

E = modulus of elasticity, psi

(d) For load displacement relationship not covered, use NB-3687.4.

NB-3690 DIMENSIONAL REQUIREMENTS FOR PIPING PRODUCTS

NB-3691 Standard Piping Products

Dimensions of standard piping products shall comply with the standards and specifications listed in Table NB-3132-1. However, compliance with these standards does not replace or eliminate the requirements of NB-3625.

NB-3692 Nonstandard Piping Products

The dimensions of nonstandard piping products shall be such as to provide strength and performance as required by this Subsection. Nonstandard piping products shall be designed in accordance with NB-3640.

VALIDATION OF THE FINITE ELEMENT STRESS ANALYSIS
COMPUTER PROGRAM CORTES-SA FOR ANALYZING PIPING
TEES AND PRESSURE VESSEL NOZZLES^{1,2}

B. R. Bass

Computer Science Division
Union Carbide Corporation
Oak Ridge, Tennessee

J. W. Bryson and S. E. Moore

Engineering Technology Division
Oak Ridge National Laboratory
Oak Ridge, Tennessee

ABSTRACT

The finite element computer program CORTES-SA, which is basically a modified version of SAP3 with a special purpose input processor for setting up a wide variety of tee joint and reinforced pressure vessel nozzle geometries, was validated by comparison of calculated stresses and displacements with results from six experimental models. During its evolution, CORTES-SA had been worked on and modified by several different people. As a consequence no single person was intimately familiar with the entire program. Validation thus required solutions for a number of problems that might be encountered in the development and/or validation of any special purpose finite element computer program. This paper presents an account of the problems encountered and the steps taken to effect their solutions. Among the problems discussed are those resulting from non-participation in the original program development; incomplete documentation at all stages of the program development; the lack of complete sets of calculated output including displacements and equilibrium forces at boundary nodes for checking purposes; the absence of adequate output graphics; and the absence of a comparable computer program for cross-checking purposes. Results from the various analytical-experimental comparison studies and other theoretical check calculations are presented.

INTRODUCTION

The ORNL Design Criteria for Piping and Nozzles Program (1-4) conducts experimental and analytical stress analysis studies of piping system components (products) to validate and/or improve design rules, criteria, and stress analysis methods for light water reactor (LWR) nuclear power-plant installations. In support of this effort, a five-program package of finite element computer programs called CORTES (California, Oak Ridge TEES), was developed at the University of California, Berkeley, specifically for stress analyses of ANSI Standard B16.9 tees subjected to internal pressure, force, moment, and thermal loadings. The

¹Research sponsored by Oak Ridge National Laboratory, operated by Union Carbide Corporation for the Energy Research and Development Administration.

²Work performed by Union Carbide Corporation for the U.S. Nuclear Regulatory Commission under Interagency Agreement 40-551-75 and 40-552-75.

program CORTES-SA (for Stress Analysis) in this group was designed to perform linear elastic stress analyses of standard tees for any one of the 13 basic mechanical loadings or an arbitrary combination of loadings (5-7). A second program, CORTES-EP (for Elastic-Plastic Analysis) has the additional capability of performing elastic-plastic analyses based on constitutive materials laws that use a von Mises yield criterion with either isotropic or kinematic hardening (8). The other programs in this group are CORTES-THFA (7) (Transient Heat Flow Analysis), SHFA (9) (Steady-state Heat Flow Analysis), and TSA (7) (Thermal Stress Analysis). All five programs feature the same automatic mesh generation routine with options that permit the modeling of a wide variety of tee-joint geometries such as tees, branch connections, and pressure vessel nozzles with a minimum of input data.

CORTES-SA has been modified several times at Oak Ridge in efforts to expand its usefulness and improve its efficiency. As a result, the present version includes contributions by a number of people in addition to the original authors. This paper describes the validation of the most recent version of CORTES-SA as released to the Argonne Code Center for general distribution. This version has been used extensively at Oak Ridge in conducting parameter studies of reinforced and unreinforced nozzles in cylindrical pressure vessels (10,11).

An account of the problems encountered and the solutions employed during the validation of CORTES-SA follows, emphasizing those experiences which should be of interest in the development and/or validation of similar special purpose numerical programs. In addition, sample results from six validation model studies are reviewed.

PROGRAM DEVELOPMENT AND VALIDATION

The CORTES package of programs was originally intended for use in stress analysis parameter studies of ANSI Standard B16.9 tees (see Fig. 1) subjected to internal pressure, force and moment loadings on the branch and run pipe extensions, and arbitrary temperature distributions. The results of these studies were to be used in conjunction with experimental studies of tees under similar loadings to develop broad-based sets of analytical results for use in confirming and/or improving design rules and structural safety criteria.

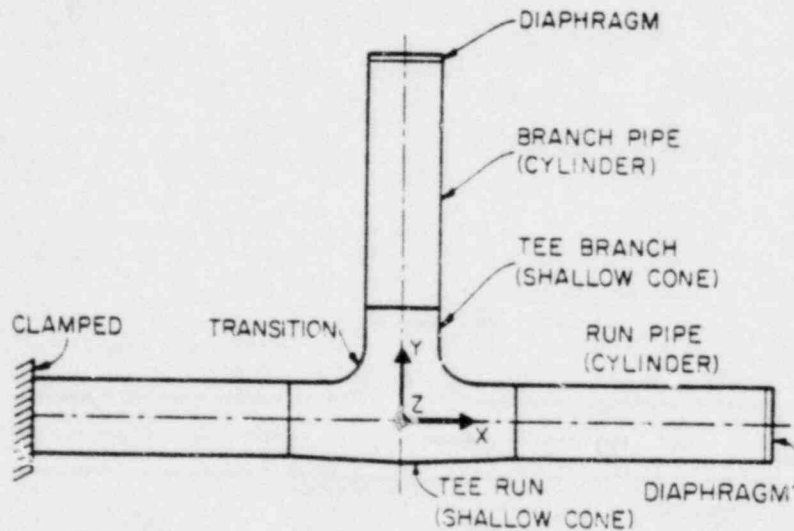


Fig. 1. Basic cylinder-to-cylinder intersection geometry.

The general guidelines for the original program development were to produce a 3-D code with isoparametric brick type elements capable of modeling a wide variety of tee joints and reinforced and unreinforced pressure vessel nozzles. Because of the anticipated usage for conducting parameter studies, automatic mesh generation with minimum input data requirements was considered to be of primary importance. The resultant program was a modified version of SAP3 (12) with a special purpose input processor that automatically models a variety of complex tee joints with several hundred finite elements, using only nine cards of input data.

Initial experiences with CORTES-SA at ORNL revealed the need for improving the input-output (I/O) efficiency and the need for certain post-processing and additional output features. Although the program automatically sets up the finite element mesh, ORNL-compatible graphics capability was needed for displaying and designing suitable mesh layouts for later stress analysis. A graphics package had been developed for use with the Oak Ridge computing facilities. Post-processing and additional graphics capability was also needed to interpret and display selected quantities from the substantial amount of output expected from large-scale parameter studies.

A second need was to augment the original output with additional information, partly for checking purposes. In the original version of CORTES-SA, the computed output consisted mainly of the surface coordinates and direction cosines of the tangent plane at the surface nodes of the generated mesh and the tangent plane stress components at the surface nodes (the model may consist of up to five layers of elements through the wall thickness). Three desirable output features not provided in the original version were the calculated displacements, the boundary node fixity conditions, and the force reactions at the fixed boundary nodes. The nodal point displacements were needed for later use in developing flexibility factors for piping system and pressure vessel analyses, whereas the other quantities were needed to validate the finite element model and computed results.

A third need was to improve the cost-time efficiency of the program at the Oak Ridge facility, which utilizes an IBM 360/195 computer rather than the CDC 6400 computer on which it was developed at the University of California. The CPU and wall clock times, core storage, and I/O requirements of large scale problems run on CORTES-SA seriously affected turnaround after job submission at the ORNL facility.

In this list of additions and modifications to SA, first priority was given to the preparation of graphics software that could be used to display the finite element models. For this purpose a software package, GRFPAK (13), was designed specifically for the CORTES input processor to display orthographic projections and cross-sectional views of the generated mesh. GRFPAK was eventually expanded to include certain node displacement and stress display options. Before the other features enumerated above could be added, the Oak Ridge computing personnel needed time to study the internal structure of the program and to design the necessary modifications. Flow diagrams and programmed comment cards would have made this job much easier.

When sufficient progress had been made on the graphics software, several models which had previously been analyzed experimentally (14-16) were analyzed for internal pressure loading and the results were compared with the experimental data. Although these initial comparisons were generally in good agreement, there was an unexplainable "spike" in the calculated stress distributions in the transverse plane (y-z plane in Fig. 1) near the nozzle-to-cylinder junction for the two thin-walled models (14,15). This stress "spike" was not present in any of the experimental data, and was not evident in the University of California results (7). The problem appeared to be related to the number and arrangement of elements in the finite element model and was less noticeable or absent for thicker walled models. Although various strategies for defining an acceptable mesh layout were attempted and numerous individuals, including the original program authors were consulted, we were not able to find an error in the program or to establish reliable guidelines to avoid the problem. By trial and error, however, we were able to generate results which did not have the spikes.

As mentioned earlier, all five programs in the CORTES package use the same finite element mesh generator, and the elastic-plastic analysis program CORTES-EP

is also capable of performing elastic analyses. There were, however, several differences between the CORTES-SA and -EP programs which made it difficult to compare results directly. First, and most importantly, the two programs calculated and output the stresses at different points in the elements. CORTES-SA printed "average" element stresses at the surface nodes expressed in the local coordinates of the tangent plane, whereas CORTES-EP printed the stress tensor components at the internal Gauss integration points expressed in global coordinates. In addition, CORTES-EP printed the node point displacement referenced to the global coordinate system. But, because of difficulties related to the use of superposition in the CORTES-SA solution logic, installation of a displacement output option in CORTES-SA had been delayed pending further study of the algorithm.

There was also an apparent difference in the mathematical formulation of the finite elements in CORTES-SA and CORTES-EP. The element originally installed in CORTES-SA (and reported in Ref. 7) was the Wilson incompatible element (17), obtained by adding nine incompatible deformation modes to the eight-node isoparametric brick element of Irons and Zienkiewicz (18). A paper by Irons et al. (19), however, pointed out that the addition of incompatible modes produces an element which violates the "patch test" and may therefore give poor results for elements that are not regular parallelepipeds. For a more complete discussion of the patch test and its importance see Ref. 20. An improved finite element which used a repair technique proposed by Taylor et al. (21) to satisfy the patch test was incorporated into CORTES-EP (8) before it was released to ORNL even though studies by Powell had failed to show any appreciable difference.

At this point in time, CORTES-EP was modified at Oak Ridge to compute and print out the tangent plane stress components at the surface nodes using a bilinear-least squares Gauss point stress extrapolation procedure developed by Hinton and Campbell (22). Using this modified version we were able to compare results directly with experimental data and with results from CORTES-SA. The spiking problem, which had been so prominent with CORTES-SA, did not materialize with CORTES-EP, and the calculated stresses showed excellent agreement with the experimental test model results. A close examination of the programming revealed, however, that the element formulations in the two programs were identical, thus eliminating the patch-test as the source of the spiking problem. Apparently, CORTES-SA had been modified earlier to conform with theory. The modification was not recorded, however, in any of the documentation supplied to ORNL by the University of California. Subsequent comparisons of stress results from CORTES-SA and CORTES-EP also eliminated the node point stress calculation routines as the source of the stress spiking problem.

Concurrently, the modification of CORTES-SA to print out surface displacements was completed. An improved matrix solving routine (borrowed from EP) was incorporated, and the standard Fortran I/O statements were replaced with local machine language routines.³ Calculations for a number of test cases were then traced through each code and compared at strategic points in the computational process. Those comparisons led to identification of a logic defect in the algorithm which automatically generates the boundary conditions for the symmetry plane nodes in CORTES-SA. The error caused one of the nodes in the y-z symmetry plane to be incorrectly restrained (fixed) for certain combinations of mesh generation parameters. When the algorithm was repaired, the excessive bending stresses at the fixed node were removed and the spike disappeared. Subsequent comparisons with experimental results, as discussed in the next section, provided sufficient evidence to claim validation for CORTES-SA.

VALIDATION MODELS AND RESULTS

During the validation process, CORTES-SA was used to analyze six models for which experimental stress analysis data were available for internal pressure loading. This set includes two thin-walled cylinder-to-cylinder models without

³ Standard Fortran I/O is retained in the version released to the Argonne Code Center.

transition fillets: ORNL-1 (14) and ORNL-3 (15); an ANSI Standard B16.9 tee: ORNL-T8 (16); a thick-walled steel pressure vessel: HSST-ITV9 (23); and two photoelastic pressure vessel models tested at Westinghouse: WC-12D and WC-100D (24). This group represents a wide range of vessel diameter-to-thickness ratios ($4.5 < D/T < 100.0$) and nozzle-to-cylinder diameter ratios ($0.1 < d_i/D_i < 0.5$), as listed in Table 1. The two thin-walled models, ORNL-1 and ORNL-3, are essentially unreinforced at the nozzle-to-cylinder transition; the B16.9 tee ORNL-T8 has a generous radius transition, while the pressure vessel models HSST-ITV9, WC-12D, and WC-100D have reinforced nozzles designed according to the rules of the ASME Boiler and Pressure Vessel Code (25), as shown in Fig. 2. In the following, comparisons between the calculated stresses from CORTES-SA and the experimental results for internal pressure loading are presented for four of the six models. Results from the other two models, ORNL-T8 and WC-100D, were equally good.

Table 1. Geometric parameters for CORTES-SA validation models

Model	D_i/T^a	d_i/t^b	d_i/D_i^c	Type of reinforcement
ORNL-1	98.0	98.0	0.5	None
ORNL-3	48.0	5.68	0.1	Extra wall thickness
ORNL-T8	32.0	21.66	0.51	ANSI B16.9, Schedule 40
HSST-ITV9	4.5	2.25	0.33	Standard
WC-12D	12.0	12.0	0.129	Standard
WC-100D	100.0	100.0	0.110	Standard

^aRatio of inner run diameter to run thickness.

^bRatio of inner branch diameter to branch thickness.

^cRatio of inner branch diameter to inner run diameter.

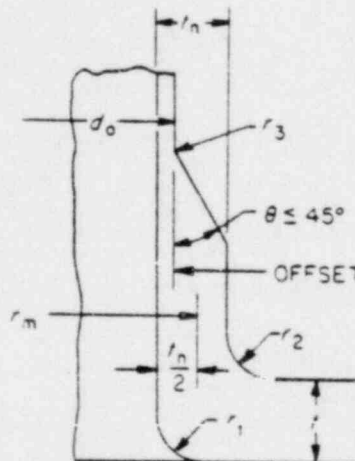


Fig. 2. ASME Code standard reinforcement design.

Cylinder-to-Cylinder Model ORNL-1

ORNL-1 is an idealized thin-shell steel structure consisting of two circular cylindrical shells ($D_i/T = 98$, $d_i/D_i = 0.5$) intersecting at right angles. There are no transitions, reinforcements, or fillets in the junction region. An isometric view of the outer surface finite element mesh is shown in Fig. 3. The finite element model was constructed using a very small fillet radius equal to 0.254 mm (0.01 in.) at the transition and one finite element through the wall

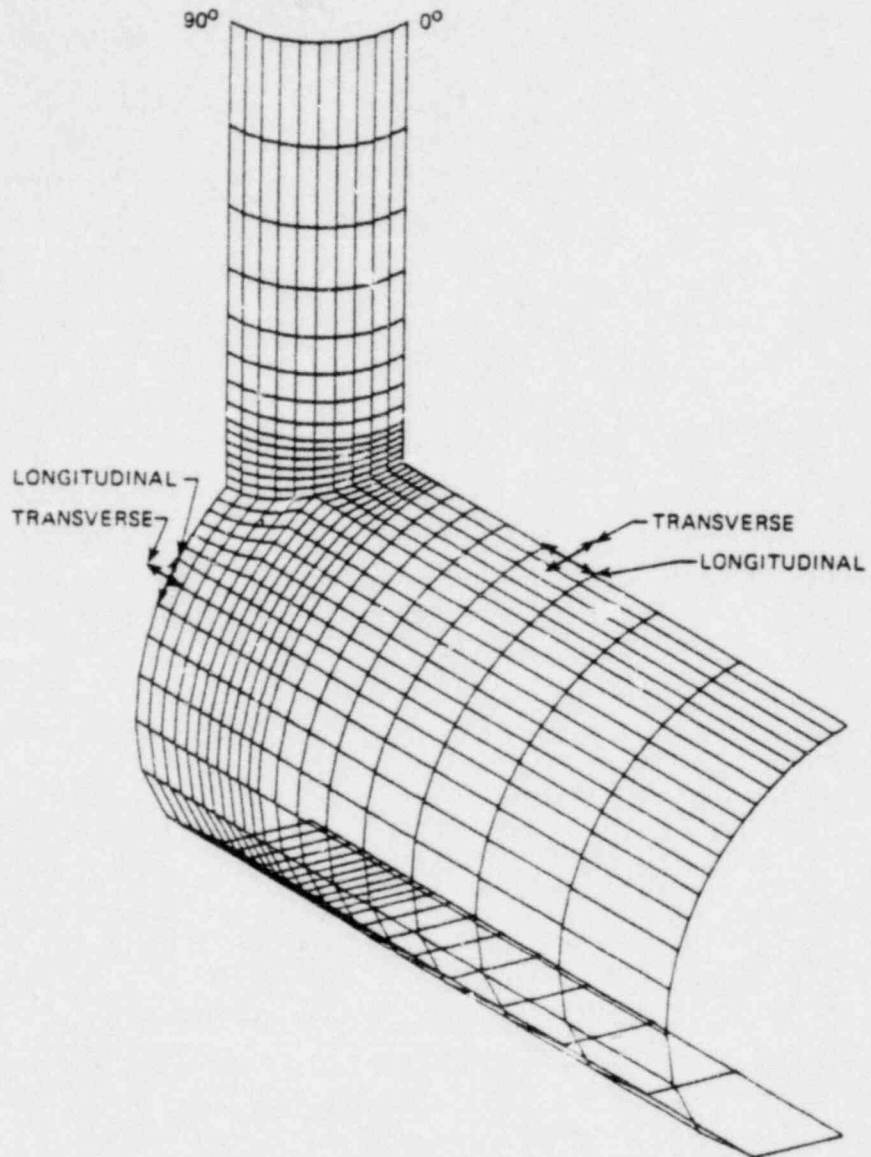


Fig. 3. Isometric view of outside surface for ORNL-1 generated mesh and definition of stresses for 0 and 90° sections.

thickness. This model was analyzed for an internal pressure of 0.345 MPa (50 psi) which produced a nominal stress of $S = PD/2T = 17.25$ MPa (2500 psi), the same as that used in the experiment.

Comparisons between the experimental data and the calculated results from CORTES-SA are depicted in Fig. 4 and 5. Longitudinal and transverse stresses (following the convention shown in Fig. 3) are shown for the 0° and 90° sections (x-y plane and y-z plane respectively) for both the inner and outer surfaces of the model. For this model the maximum stress was in the transverse direction in the longitudinal plane (0° section) at the outer surface of the intersection.

In general, the computed results from CORTES-SA are in good agreement with the experimental data. The relative disagreements shown in Figs. 5(c) and 5(d) for the 90° section (y-z plane) of the run pipe are the result of using isoparametric brick type elements to analyze thin-walled structures, as pointed out in Ref. 26. For thicker walled structures, like ORNL-3 discussed below, CORTES-SA gives better agreement with experimental data in this region.

Cylinder-to-Cylinder Model ORNL-3

ORNL-3 is the second tee joint for which experimental and analytical results from CORTES-SA were compared. ORNL-3 is also an idealized thin-shell structure with no transitions, reinforcements, or fillets in the junction region. In contrast with ORNL-1, however, ORNL-3 has a much smaller diameter ratio ($d_i/D_i = 0.1$ vs 0.5) and a greater relative wall thickness ($D_i/T = 48$ vs 98). Results from this model shed light on the ability of CORTES-SA to accurately predict stresses for models with small relative nozzle diameters (d_i/D_i ratios) like those used in many pressure vessels.

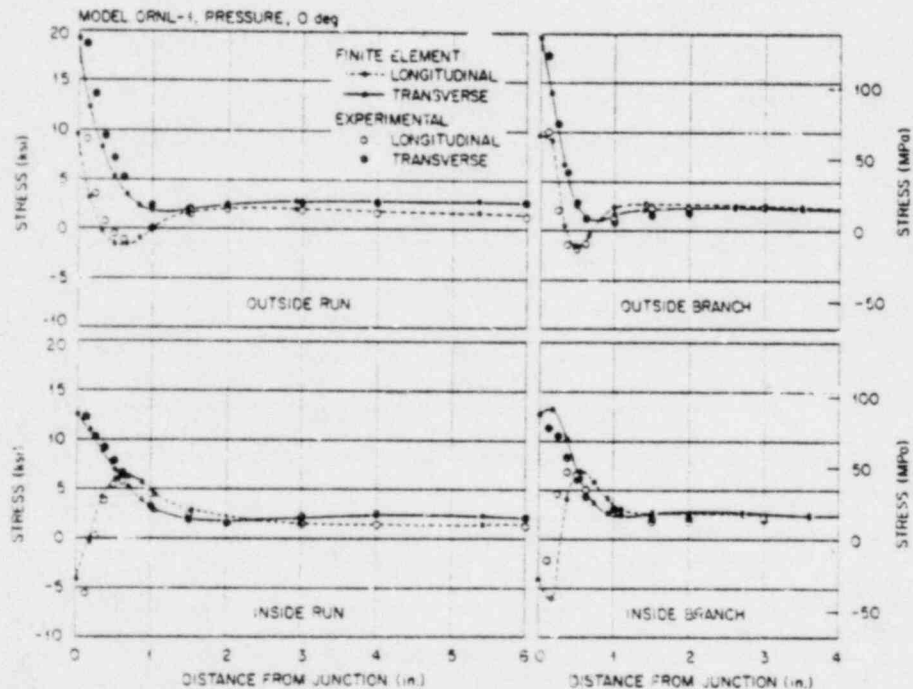


Fig. 4. Comparisons of calculated and experimental stress distribution for 0° section of model ORNL-1 (1 in. = 25.4 mm).

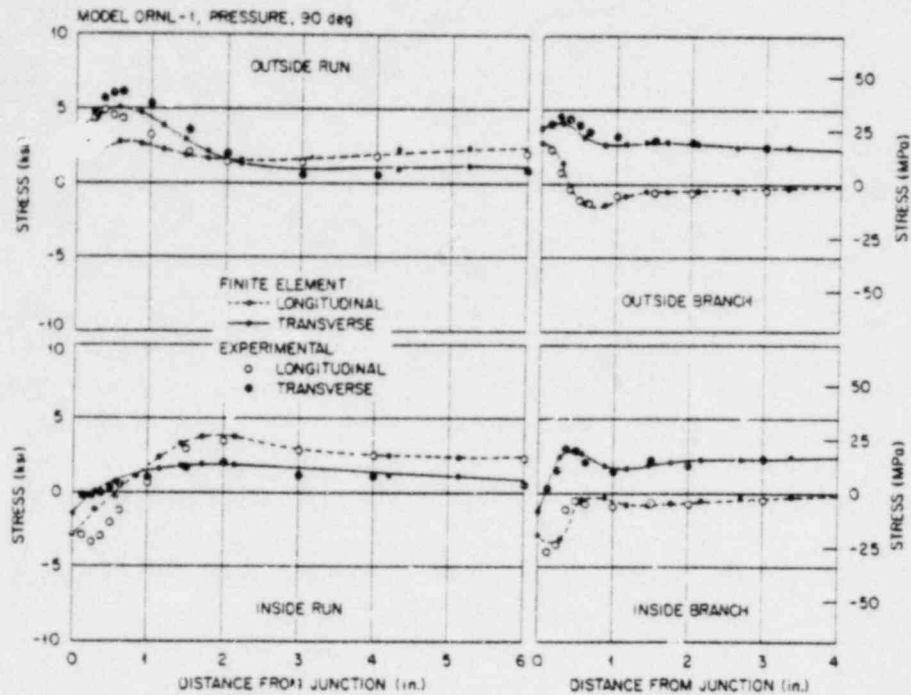


Fig. 5. Comparisons of calculated and experimental stress distributions for 90° section of model ORNL-1 (1 in. = 25.4 mm).

Figure 6 shows the outer surface of the finite element mesh, constructed like the model for ORNL-1, with a very small fillet at the junction. The mesh layout for ORNL-3 utilizes two elements through the wall thickness. The number of elements through the wall thickness for this model, as well as for the other test cases, is governed by the criterion that the elements in the junction region should be as nearly cubical in shape as possible, consistent with the selected degree of mesh refinement in the axial and circumferential directions of the branch and run. The model was analyzed with an internal pressure of 2.068 MPa (300 psi) or a nominal stress of $S = 50.67$ MPa (7350 psi).

Comparisons between the experimental and analytical results are shown in Figs. 7 and 8 for the 0° and 90° sections, respectively. The maximum stress for ORNL-3 is in the transverse direction in the longitudinal plane at the inner surface of the intersection.

Westinghouse Photoelastic Model WC-12D

To demonstrate the capability of CORTES-SA to analyze reinforced pressure vessel nozzle configurations, comparisons between the experimental and analytical results are presented for one of the two photoelastic models tested by Leven (24), WC-12D, and for the HSST vessel ITV9. The photoelastic model WC-12D had a relative nozzle size ($d_i/D_i = 0.129$) near that of ORNL-3 but with reinforcement as prescribed by the ASME Boiler and Pressure Vessel Code shown earlier in Fig. 2. The vessel was relatively thick-walled with a diameter-to-thickness ratio of $D_i/T = 12.0$.

All of the test cases which were reinforced in the junction region, including WC-100D which is not shown here and the HSST model discussed below, required

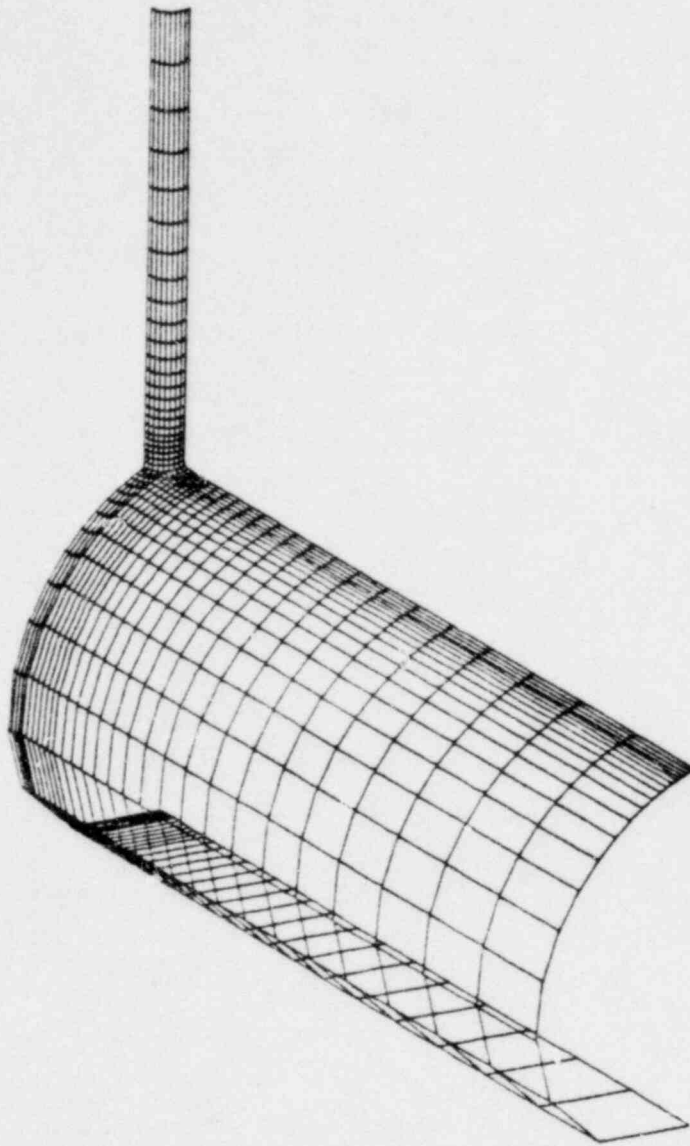


Fig. 6. Isometric view of outside surface for ORNL-3 generated mesh.

more elements through the wall thickness than were needed for the unreinforced models. Model WC-12D was analyzed using three layers of elements. Since WC-12D was a photoelastic model, the finite element analysis was initially performed using material property values of $E = 51.7 \text{ MPa}$ (7500 psi) and Poisson's ratio of $\nu = 0.485$. A second analysis was also made using material constants $E = 206.8 \text{ GPa}$ ($30 \times 10^6 \text{ psi}$) and $\nu = 0.3$ (steel properties). An internal pressure of 1.061 MPa (153.9 psi) was used for the analyses for a nominal stress of $S = 6.895 \text{ MPa}$ (1000 psi).

Comparisons between the computed results and the experimental data are shown in Figs. 9 and 10. Good agreement was obtained between the calculated results for the photoelastic and the steel models except in the junction region

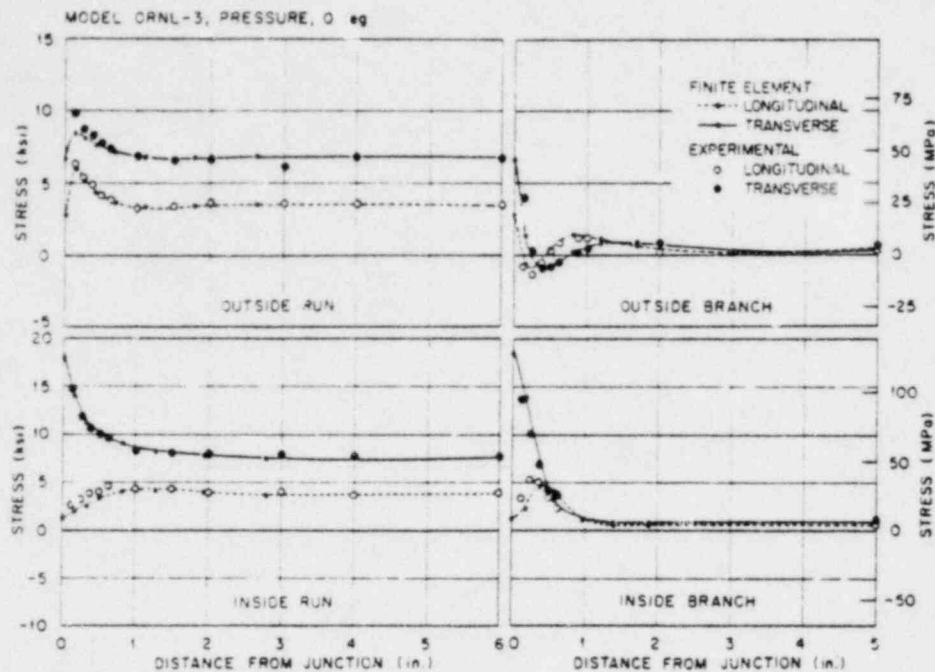


Fig. 7. Comparisons of calculated and experimental stress distributions for 0° section of model ORNL-3 (1 in. = 25.4 mm).

of the 0° section. In this section, the results of the steel analysis compare very favorably with the experimental data, whereas the computed photoelastic results are not as good.

The discrepancy in the photoelastic calculation for the 0° section reflects the difficulties encountered in using the conventional finite element displacement formulation (the formulation used in CORTES-SA) to analyze structures of nearly-incompressible materials (see, for example, Ref. 27). This displacement formulation, which is derived from the minimum potential energy principle, can yield stress results greatly in error as Poisson's ratio approaches $1/2$, i.e., as the material approaches incompressibility. In the limiting case, i.e., $\nu = 1/2$, the formulation is no longer valid. Computationally, the global stiffness matrix becomes progressively more ill-conditioned until it becomes singular at $\nu = 1/2$ (28). For discussions of modified variational formulations that are applicable to near incompressible and incompressible materials, see papers by Malkus (29), Booker et al. (30), and Taylor et al. (31).

Intermediate Test Vessel HSST-ITV9

Of the six models analyzed, the Heavy Section Steel Technology Program intermediate test vessel HSST-ITV9 had the greatest relative wall thickness and nozzle diameter with dimensional ratios of $D_1/T = 4.5$ and $d_1/D_1 = 0.33$. Both the experimental and finite element analyses performed on HSST-ITV9 used an internal pressure of 6.895 MPa (1000 psi).

The finite element model for HSST-ITV9 was constructed using four layers of elements through the wall thickness. The calculated stresses for this model are indicated by the solid data points in Figs. 11 and 12 for the 0° and 90° planes respectively. Experimental data, from Ref. 23, are indicated by the open data points for the inside corner of the nozzle in both planes and for the outside fillet in the 0° plane. The maximum stress for this model occurred at the inside corner in the longitudinal (0°) plane.

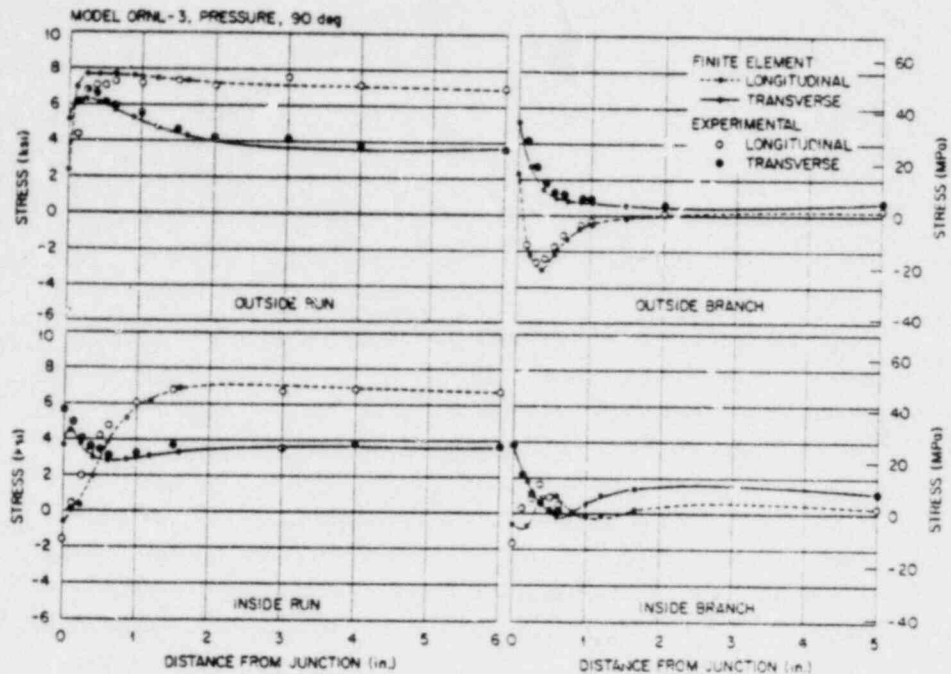


Fig. 8. Comparisons of calculated and experimental stress distributions for 90° section of model ORNL-3 (1 in. = 25.4 mm).

As illustrated in Figs 4 through 12, generally good agreement was obtained between the calculated stresses and the experimental data for the validation models. The calculated maximum stress and stress distributions for both the longitudinal plane (0° section) and the transverse plane (90° section) closely follow the experimental data with the exception of two cases previously noted. These exceptions pertain either to a thin-walled structure (ORNL-1) for which the finite element formulation in CORTES-SA is only marginal; or to the nearly incompressible behavior of photoelastic materials (WC-12D) for which the finite element formulation tends to become unstable. In summary, we consider the correlations to be sufficiently accurate, within the constraints noted, to claim validation for CORTES-SA.

SUMMARY AND CONCLUSIONS

In this paper we have described the validation process conducted at ORNL for the special purpose finite element computer program CORTES-SA and have presented comparison results for four of six models that were extensively studied. The discussions have focused mainly on the problems encountered during a development and expansion phase to make the program more useful and a validation phase to prove the value of the program. Some of the major points, which proved to be crucial for the validation of CORTES-SA, are reviewed below from the perspective of general program development.

During the development phase of special purpose computer codes such as CORTES-SA, the program output should be carefully designed to make available all of the information needed to completely define the model being analyzed, perhaps under control of an output option. It is well to note that output requirements for validation of the program will probably be more extensive than required for later production use, but the option should still be available for later checking. In the case of CORTES-SA, the boundary point fixity conditions, the boundary point reaction forces, and the computed node point displacements were needed to

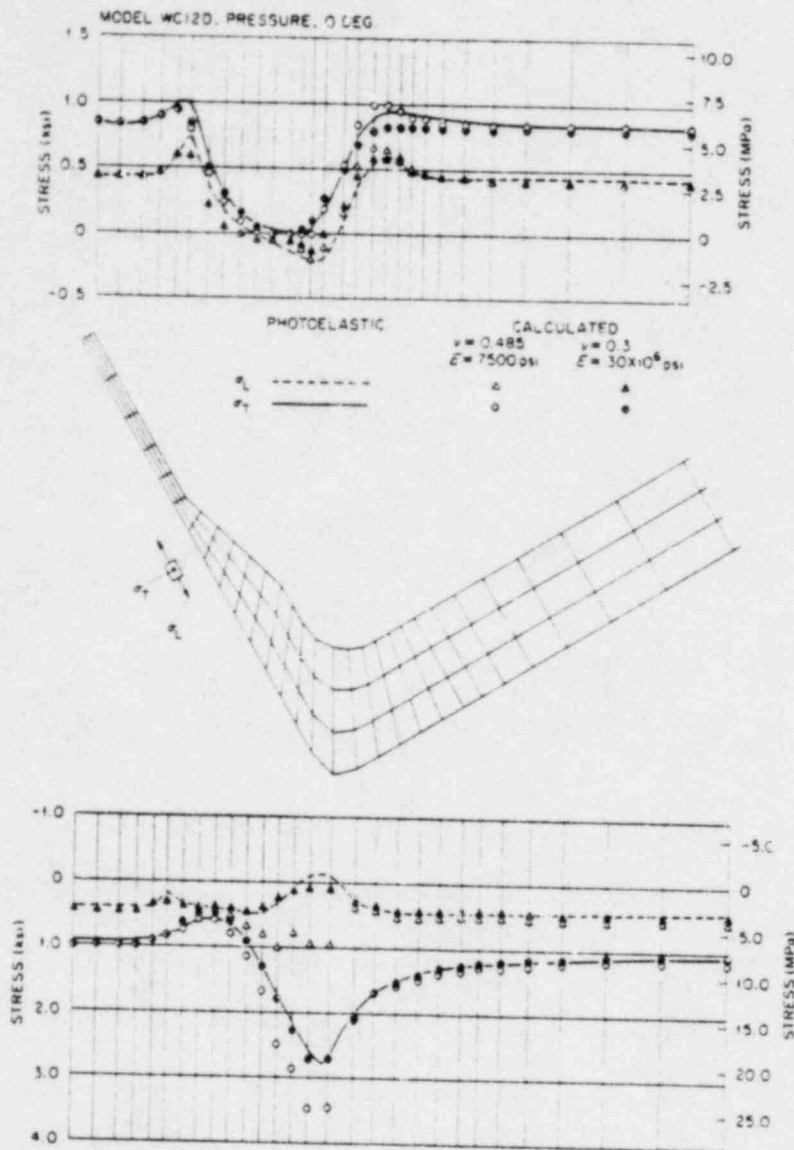


Fig. 9. Comparisons of photoelastic and calculated stress distributions for 0° section of model WC-12D.

insure that the program was generating the correct boundary conditions. Much of this information is not needed for the parameter study discussed in Refs. 10 and 11.

A second topic of importance concerns the impact of graphics software on program validation. For finite element programs like CORTES-SA that generate complex mesh geometries automatically, graphical displays play an important role in finalizing the design of the element mesh to be analyzed. For example, the accuracy of the finite element formulation used in CORTES-SA may be adversely affected by mesh layouts not composed primarily of parallelepipeds. Although it is not possible to construct a mesh layout of perfect parallelepipeds, by examining isometric and cross-sectional plots of successive trial models generated

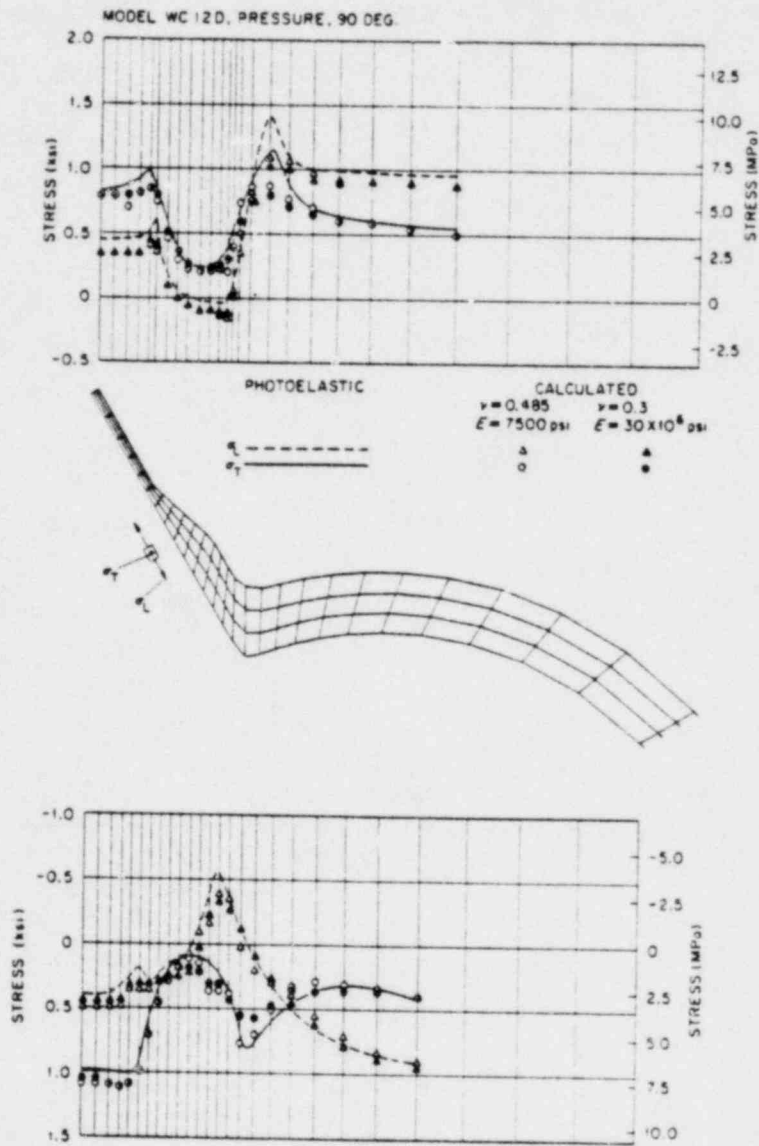


Fig. 10. Comparisons of photoelastic and calculated stress distributions for 90° section of model WC-12D.

by SA, it becomes rather easy to construct suitable finite element models for each case. (It was also easier to make minor changes in the mesh generation package.) The availability of additional graphics software with selected stress and displacement plotting capability also makes possible quick and accurate analysis of the large quantity of output from the solution process. Much of the information currently available from CORTES-SA analyses would be extremely difficult to assimilate and interpret without the graphics software.

Another important consideration in the development and validation process concerns documentation. External documentation, including flow diagrams and a complete log of modifications and updates to the program as well as user instructions, should be conscientiously maintained. Such practice will enable successive users of the program to be brought up to date quickly and will provide the

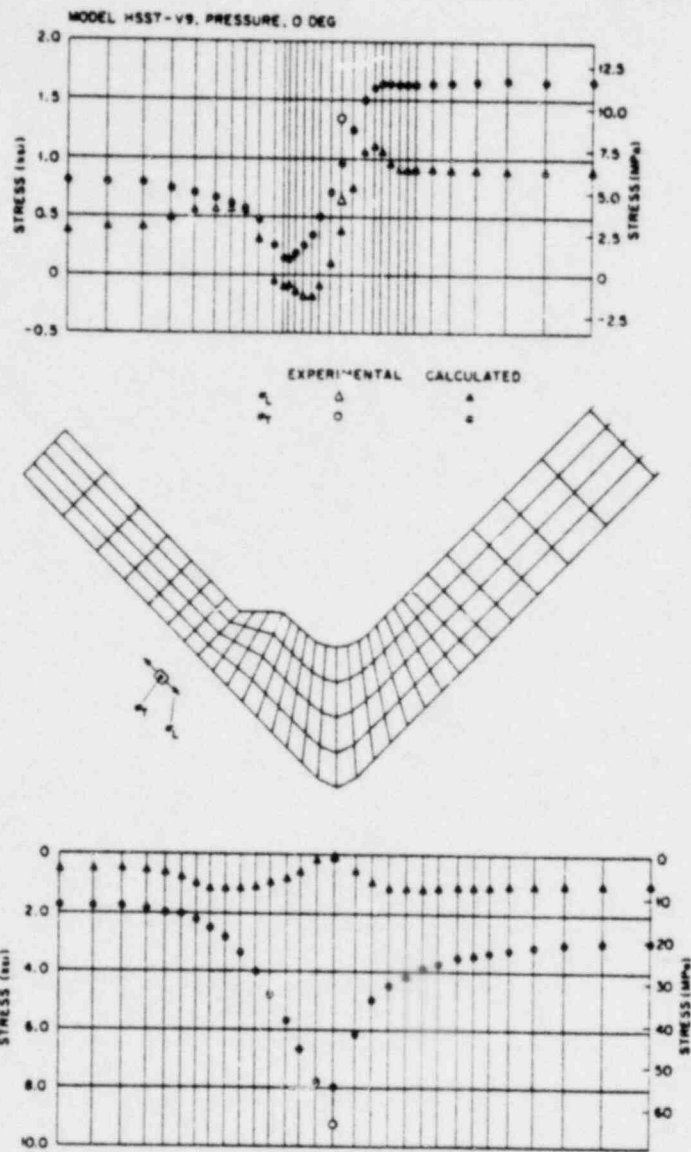


Fig. 11. Calculated stress distributions for 0° section of model HSST-ITV9.

experienced users with a permanent record. In our case, CORTES-SA was modified several times by different people after it had been delivered, and different versions of the program were often in use at any given time.

Adequate internal documentation, in the form of programmed comment cards should be included during the development phase and conscientiously maintained at each modification. Full internal documentation can be of great assistance either in modifying the program or in locating errors and defects in the algorithms.

Finally, we offer some comments concerning our interpretation of the validation procedure. In validating a special purpose program, it is desirable to have a second code (usually a general purpose program) available for

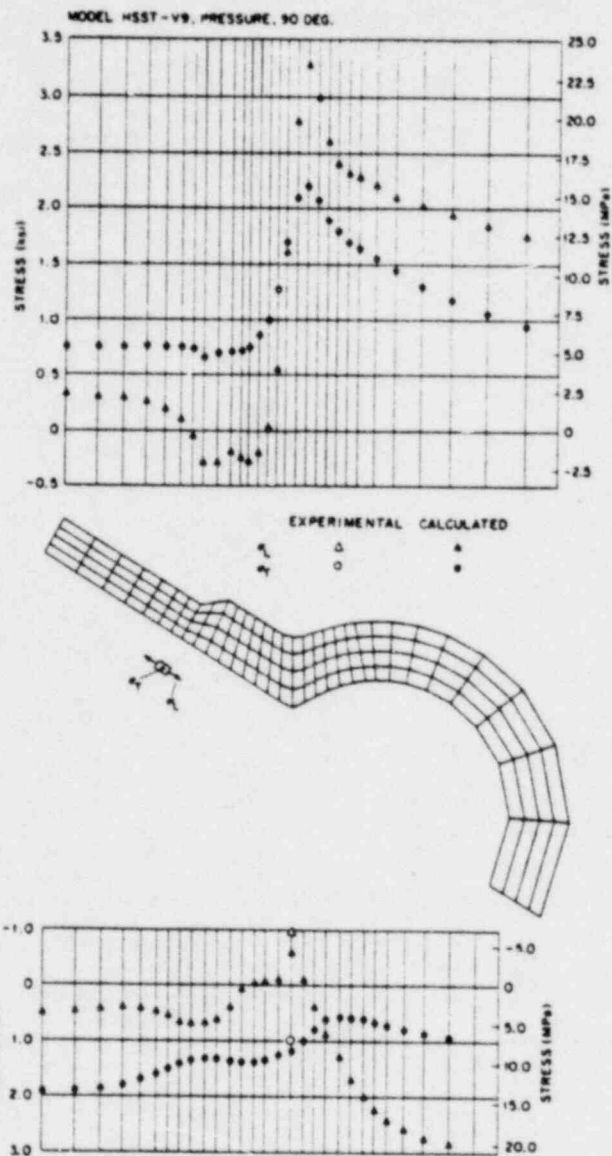


Fig. 12. Calculated stress distributions for 90° section of model HSST-ITV9.

comparative analyses of test problems. The experience with CORTES-SA demonstrates clearly, however, that such a check may not constitute a true validation of the program in the absence of comparisons with well documented experimental data. In particular, the stress-spiking defect in CORTES-SA would probably not have been corrected and the program not properly validated had the experimental data not been available for comparison. Such computational-experimental comparison studies provide the best assurance for a reliable computer program validation.

In our opinion the finite element computer program CORTES-SA is fully validated for the elastic stress analysis of cylinder-to-cylinder tee joints, ANSI Standard B16.9 tees, and single reinforced and unreinforced nozzles in cylindrical pressure vessels. The favorable comparisons with well documented

experimental data over a wide range of geometric parameters supports this conclusion. In addition, the minimal amount of required input (nine cards) and the available graphics software for both pre- and post-processing should make CORTES-SA, as well as the other CORTES programs, all of which may be obtained through the Argonne Code Center, a valuable set of analytical tools for the safe design of nuclear power plant pressure vessels and piping systems.

REFERENCES

1. Greenstreet, W. L., Moore, S. E., and Callahan, J. P., *Fourth Annual Progress Report on Studies in Applied Solid Mechanics (Pressure Vessels and Piping System Components)*, ORNL-4925, July 1974.
2. Moore, S. E. and Bryson, J. W., "Design Criteria for Piping and Nozzles," in *FY 1976 Annual Report of Contract Research for the Metallurgy and Materials Research Branch, Division of Reactor Safety Research*, NUREG-0185, U.S. Nuclear Regulatory Commission, Feb. 1977.
3. Greenstreet, W. L., "Summary and Accomplishments of the ORNL Program for Nuclear Piping Design Criteria," *Proceedings of the Technology Information Meeting on Methods for Analysing Piping Integrity*, ERDA 76-50, Nov. 11-12, 1975.
4. Moore, S. E., "Contributions of the ORNL Piping Program to Nuclear Piping Design Codes and Standards," *Journal of Pressure Vessel Technology*, Vol. 99, Feb. 1977, pp. 224-236.
5. Powell, G. H., Clough, R. W., and Gantayat, A. N., *Stress Analysis of B16.9 Tees by the Finite Element Method*, ASME Paper 71-PVP-40, May 1971.
6. Clough, R. W., Powell, G. H., and Gantayat, A. N., "Stress Analysis of B16.9 Tees by the Finite Element Method," Paper F4/7, *First International Conference on Structural Mechanics in Reactor Technology*, Berlin, Germany, Sept. 20-24, 1971.
7. Gantayat, A. N. and Powell, G. H., *Stress Analysis of Tee Joints by the Finite Element Method*, University of California Report UC-SESM-73-6, ORNL/Sub/3193-1, Feb. 1973.
8. Powell, G. H., *Finite Element Analysis of Elasto-Plastic Tee Joints*, University of California Report UC-SESM-74-14, ORNL/Sub/3193-2, Sept. 1974.
9. Textor, R. E., *User's Guide for SHFA: Steady-State Heat Flow Analysis of Tee Joints by the Finite Element Method*, UCCND/CSD/INF-60, Jan. 1976.
10. Bryson, J. W., Johnson, W. G., and Bass, B. R., *Stresses in Reinforced Nozzle-Cylinder Attachments Under Internal Pressure Loading Analysed by the Finite Element Method - A Parameter Study*, ORNL/NUREG-4 (to be published).
11. Bryson, J. W., Johnson, W. G., and Bass, B. R., *Stresses in Reinforced Nozzle-Cylinder Attachments Under External Moment Loadings Analysed by the Finite Element - A Parameter Study* (to be published).
12. Wilson, E. L., *Finite Element Analysis of Mine Structures*, University of California Final Report to DOI, Contract No. H0110231, Sept. 1972.
13. Fowler, P. G. and Bryson, J. W., *User's Manual for the CORTES Graphics Package GRFFAK* (to be published).
14. Corum, J. M., et al., *Theoretical and Experimental Stress Analysis of ORNL Thin-Shell Cylinder-to-Cylinder Model No. 1*, ORNL-4553, Oct. 1972.
15. Gwaltney, R. C., *Theoretical and Experimental Stress Analysis of ORNL Thin-Shell Cylinder-to-Cylinder Model No. 3*, ORNL-5020, June 1975.
16. Moore, S. E., Weed, R. A., and Grigory, S. C., *Experimental Elastic-Response and Fatigue to Failure Tests of Pivs 12-in. Nominal Size ANSI Standard B16.9 Tees*, ORNL/NUREG-3 (to be published).
17. Wilson, E. L., Taylor, R. L., Doherty, W. P., and Ghaboussi, J., "Incompatible Displacement Models," *Numerical and Computer Methods in Structural Mechanics* (ed. S. J. Fenves et al), Academic Press, New York, 1973, pp. 46.
18. Irons, B. M. and Zienkiewicz, O. C., "The ISO Parametric Element System - A New Concept in Finite Element Analysis," *Proceedings, Conference on Recent Advances in Stress Analysis*, Royal Aeronautical Society, London, England, 1968.
19. Irons, B. M., Olivera, E. R., and Zienkiewicz, O. C., "Comments on the Paper 'Theoretical Foundations of the Finite Element Methods,'" *Int. J. Solids Structures*, Vol. 6, 1970.

20. Strang, G. and Fix, G. J., *An Analysis of the Finite Element Method*, Prentice-Hall, Englewood Cliffs, N.J., 1973.
21. Taylor, R. L., Beresford, P. J., and Wilson, E. L., "A Non-Conforming Element for Stress Analysis," *Int. J. Num. Meth. Eng.*, Vol. 10, 1976, pp. 1211-1219.
22. Hinton, E. and Campbell, J. S., "Local and Global Smoothing of Discontinuous Finite Element Functions Using a Least Squares Method," *Int. J. Num. Meth. Eng.*, Vol. 8, 1974, pp. 461-480.
23. Merkle, J. G., Robinson, G. C., Holz, P. P., and Smith, J. E., *Test of 8-In.-Thick Pressure Vessels. Series 4: Intermediate Test Vessels V-6 and V-9, with Inside Nozzle Corner Cracks*, ORNL/NUREG-7 (to be published).
24. Leven, M. M., *Stress Distribution at Two Closely-Spaced Reinforced Openings in a Pressurized Cylinder*, Research Report 71-9E7-PHOTO-R1, Westinghouse Research Laboratories, Apr. 1971.
25. *ASME Boiler and Pressure Vessel Code, Section III, Div. 1, "Nuclear Power Plant Components"*, American Society of Mechanical Engineers, New York, 1974.
26. Irons, B. M. and Hellen, T. K., "On Reduced Integration in Solid Isoparametric Elements When Used in Shells with Membrane Modes," *Int. J. Num. Meth. Eng.*, Vol. 10, 1976, pp. 1179-1182.
27. Hermann, L. R. "Elasticity Equations for Incompressible and Nearly Incompressible Materials by a Variational Theorem," *AIAA J.*, Vol. 3, No. 10, 1965, pp. 1896-1900.
28. Fried, I., "Influence of Poisson's Ratio on the Condition of the Finite Element Stiffness Matrix," *Int. J. Solids Structures*, Vol. 9, 1973, pp. 323-329.
29. Malkus, D. S., "A Finite Element Displacement Model Valid for Any Value of the Compressibility," *Int. J. Solids Structures*, Vol. 12, 1976, pp. 731-738.
30. Booker, J. R. and Small, J. C., "The Economical Solution of Elastic Problems for a Range of Poisson's Ratio," *Int. J. Num. Meth. Eng.*, Vol. 9, 1975, pp. 847-853.
31. Taylor, R. L., Pister, K. S., and Hermann, L. R., "On a Variational Theorem for Incompressible and Nearly-Incompressible Orthotropic Elasticity," *Int. J. Solids Structures*, Vol. 4, 1968, pp. 875-883.

reprinted from

Pressure Vessel and Piping Computer Program Evaluation and Qualification, PVP-PB-024

Edited by D. E. Dietrich, 1977

published by

THE AMERICAN SOCIETY OF MECHANICAL ENGINEERS

345 East 47th Street, New York, N.Y. 10017

Printed in U.S.A.